Western Kentucky University
TopSCHOLAR®

Masters Theses & Specialist Projects | Graduate School

11-1-1971

Thermionic Space Charge Oscillations

William Carl
Western Kentucky University

Follow this and additional works at: http://digitalcommons.wku.edu/theses

 Part of the Physics Commons

Recommended Citation
Carl, William, "Thermionic Space Charge Oscillations" (1971). *Masters Theses & Specialist Projects.* Paper 1038.
http://digitalcommons.wku.edu/theses/1038

This Thesis is brought to you for free and open access by TopSCHOLAR®. It has been accepted for inclusion in Masters Theses & Specialist Projects by an authorized administrator of TopSCHOLAR®. For more information, please contact connie.foster@wku.edu.

[illegible]

THERMIONIC SPACE CHARGE OSCILLATIONS

BY

WILLIAM L. CARL

A THESIS

SUBMITTED IN PARTIAL FULFILLMENT

OF THE REQUIREMENTS FOR THE DEGREE OF

MASTER OF SCIENCE IN ENGINEERING PHYSICS

WESTERN KENTUCKY UNIVERSITY

NOVEMBER, 1971

THERMIONIC SPACE CHARGE OSCILLATIONS

Richard J. Komp

Thesis Advisor: Dr. Richard Komp
Department of Physics and Astronomy
Western Kentucky State University

Floyd M. Curtis

W. Frank Fix

L. J. Sanderson

Dean of Graduate School

ABSTRACT

THERMIONIC SPACE-CHARGE OSCILLATIONS

Thermionic electrons emitted into a potential well will produce radiation, the frequency of which is determined by the transit time of the electrons. This paper investigates the case where radiation is produced by a vacuum tube in which two Pierce guns face each other, one acting as the emitter, the other acting as a reflector. Symmetry and the focusing of the electron beam by the Pierce guns make it possible to make an accurate determination of the electron transit time.

Measurements showed that the period of the oscillation was 1.5 times the period required for an electron to traverse the well and return to the emitting cathode. Attempts to account for this period by presently accepted modes of oscillation were unsuccessful.

A model developed to explain the observations resulted from establishing compatibility of the electron flow in the emitter and the cathode-accelerator space. A conclusion drawn from the model is that conventional calculations of the emitted current density should be modified to account for the shift in energy levels of the electrons in the emitter as a result of the surface-directed electron drift.

ACKNOWLEDGMENTS

I would like to acknowledge the very valuable assistance and guidance given me in the preparation of this thesis by Dr. Richard Komp, of Western Kentucky State University. I also appreciate the careful review and suggestions of Dr. John Richardson, of the General Electric Company.

TABLE OF CONTENTS

TABLE OF CONTENTS--CONTINUED

LIST OF TABLES

LIST OF ILLUSTRATIONS

LIST OF ILLUSTRATIONS--CONTINUED

INTRODUCTION

Barkhausen Oscillations Discovered

In 1920, H. Barkhausen and K. Kurz (1) announced a new way to generate ultrahigh frequency radio waves. The Barkhausen-Kurz oscillator was a three-electrode vacuum tube which had a filamentary emitter, an accelerating electrode which was semitransparent to electrons, and a solid reflecting electrode. Barkhausen explained that the radiation resulted from oscillation of the electrons about the plane of the accelerating electrode. Barkhausen stated that the necessary criteria for oscillation were:

1) The filament had to be operated such that its emission would be temperature limited.
2) The electrodes had to be cylindrical.
3) Tuned impedances had to be used in the circuits of the electrodes, but the frequency of the oscillations was independent of the frequencies of the tuned circuits and was a function only of the potentials applied to the tube.

Although his tubes had cylindrical geometries, Barkhausen assumed planar geometries in calculating the frequency of the oscillation. Because his filament was

operating temperature limited, Barkhausen assumed that the influence of space charge was negligible and that the potential gradients in his tubes were linear. Figure 1 illustrates the model Barkhausen used in calculating the frequency of oscillation.

From the geometry of Figure 1,

$$d' = \frac{E_g d_a - E_a d_g}{2(E_g - E_a)}$$

where d' is the distance from the filament to the point where the potential becomes zero and the electrons are reflected; d_g is the diameter of the accelerator grid; d_a is the diameter of the reflector; E_g is the potential of the accelerator; and E_a is the potential of the reflector. The distance that an electron travels in one cycle is 2d'.

The average velocity of the electrons is given by

$$v(\text{average}) = \sqrt{\frac{eE}{2m}g}$$

where v(average) is the average velocity in meters per second, and m is the mass of the electron in kilograms. The frequency of the oscillations is given by the average velocity divided by the distance the electrons travel:

$$n = \frac{v(\text{average})}{2d'} = \frac{\sqrt{\frac{eE}{2m}g}}{\frac{E_g d_a - E_a d_g}{(E_g - E_a)}}$$

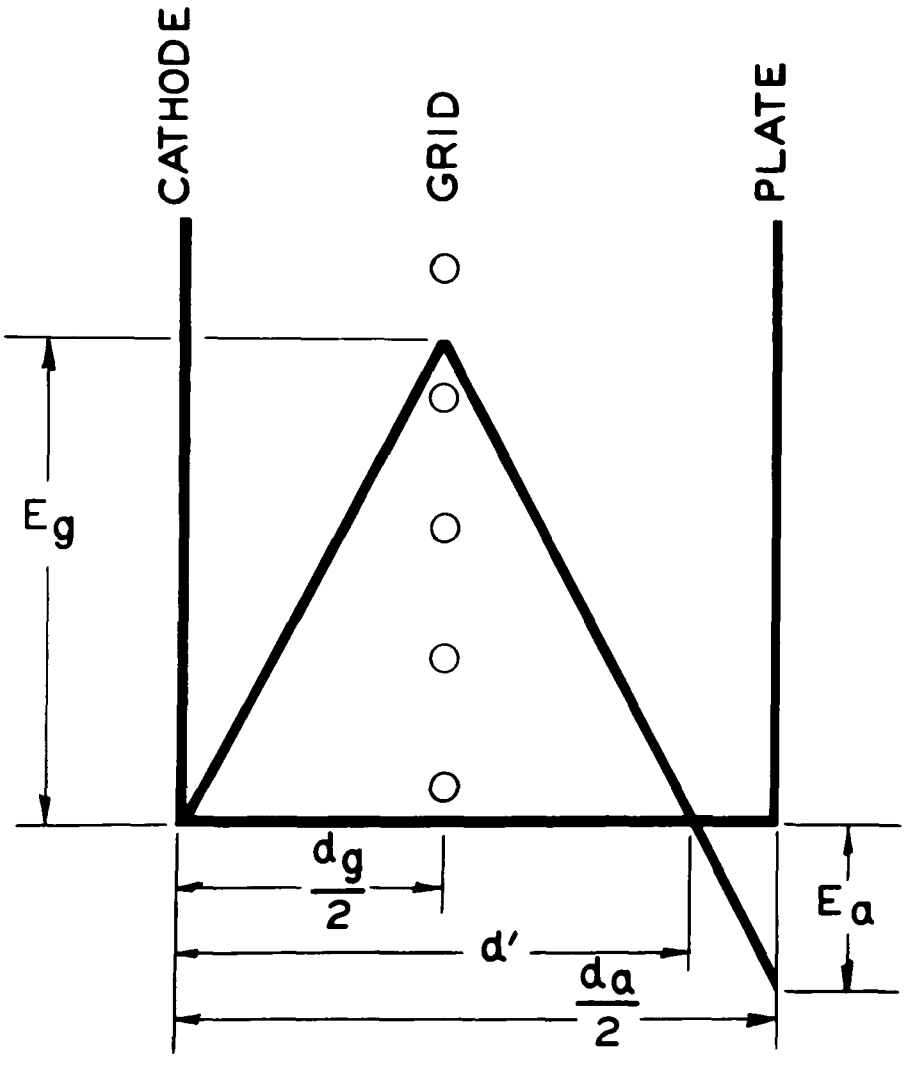

$$d' = \frac{E_g d_a - E_a d_g}{2(E_g - E_a)}$$

$$V_{aver} = \sqrt{\frac{1e}{2m} E_g}$$

$$n = \frac{\sqrt{\frac{1e.}{2m} E_g}}{\frac{E_g d_a - E_a d_g}{E_g - E_a}}$$

BARKHAUSEN'S DERIVATION BASED ON THE ILLUSTRATED POTENTIAL DISTRIBUTION IN THE OSCILLATOR

FIG. 1

Although the simple model assumed by Barkhausen differed substantially from the actual devices, there was relatively good agreement between calculated and measured values of the frequency.

Further Investigation And Efforts to Enhance Oscillation

Starting with Barkhausen's results, many investigators began experimenting with retarding-field oscillators. In these investigations, each of the criteria for oscillation cited by Barkhausen were subsequently found to be invalid.

By 1922, E. W. Gill and J. H. Morrell (2) reported that under some conditions the external circuit did influence the frequency of oscillations. In 1934, W. H. Moore (3) reported on oscillations from retarding-field tubes in which no tuned circuits were used. Test results on eleven tubes were reported in Moore's paper. One of these tubes oscillated before the cathode current became temperature limited, and this anomaly was cited by Moore. In his paper, Moore investigated the accuracy of wave length equations developed by A. Scheibe (4), H. E. Hollmann (5), and T. V. Jonescu (6) as well as the wave length equation developed by Barkhausen and Kurz. The relations which agreed best with the results were the Barkhausen-Kurz relation and the Scheibe relation, which is basically the Barkhausen-Kurz relation modified to account for the fact that the geometry of the tubes was

cylindrical rather than planar. The measured wave lengths were shorter than the values predicted by the calculations. No tube dimensions were given in the paper.

Also in 1934, B. J. Thompson and P. D. Zotto (7) reported finding that a tube having planar electrodes could be made to oscillate if a solid electrode, having a potential negative with respect to the filament, was placed on the side of the filament wires opposite the accelerating electrode.

In 1934, L. F. Dytrt (8) reported oscillations from a tube in which the reflector was operated at a potential which was positive with respect to the filament. Thus, all of the criteria postulated from the original model have been shown to be invalid through experimental results.

F. B. Llewellyn (9, 10) published two important papers in which he developed his classic method of analyzing electronic motion. Llewellyn's application of his analytical techniques to the Barkhausen oscillator was the most rigorous and sophisticated publication of attempts to analyze the mechanism of the oscillation. However, after a series of communications with W. E. Benham, England, Llewellyn concluded that his analysis of the negative-plate oscillator, in which electrons were returned toward the filament, was invalid.

The introduction of the klystron in 1938 attracted attention away from the relatively-inefficient and difficult-to-control Barkhausen-Kurz oscillators, and reports of

investigations of efforts to improve operation and understanding of the devices virturally disappeared from the literature. However, as late as 1952, J. J. Ebers (11) reported oscillation at 6,000 MHz with an over-all efficiency of 4.5 per cent from an improved-design, retarding-field oscillator in which a resonant cavity coupled with the accelerator and reflector electrodes.

Efforts to Eliminate Oscillation

It is ironic that for almost twenty years after its invention there was a substantial effort made by technical investigators in trying to enhance the generation of high-frequency radiation from Barkhausen oscillators; yet, following the introduction of television in the 1940s, there has been an additional twenty years of effort in trying to prevent Barkhausen oscillations in tubes performing television functions where the generation of high-frequency radiation by tubes in the receiver interfere with the incoming signal. It was in this latter effort that the writer became involved in the study of Barkhausen oscillations.

It was found that an acceptable theory of oscillation in a potential-well type of tube in the absence of tuned feed-back circuits had not been formulated. One could accept intuitively the theory that the radiation was caused by the oscillation of swarms of electrons

about the plane of the accelerating electrode ; but, there were no mathematical relationships which were suitable for application to the problem.

The original Barkhausen model was completely unacceptable because in it the effects of space charge were assumed to be negligible. Most of the television radiation problems are created by beam tetrodes used in the horizontal-sweep function. In these tubes, the radiation is generated while the anode, which would correspond to the reflector in the Barkhausen model, is at a substantial positive potential. The reflection, under these circumstances, occurs at a virtural cathode which is established between the screen grid and the anode, as illustrated in Figure 2.

In reporting the results of an extensive investigation of objectionable radiation from beam tetrodes, D. Hoogmoed and A. J. Huart (12) empirically concluded that the radiation was probably caused by Barkhausen-like oscillation of charge. It was assumed that the electrons were reflected by the virtual cathode established between the screen grid and the anode. However, there was no mathematical model for use in calculating the theoretical frequency, other than the original Barkhausen-Kurz relation. Furthermore, Hoogmoed and Huart noted that there should be no radiation from arbitrarily oscillating electrons. Unless there was a mechanism which would cause the electrons to "bunch," there would be no radiation.

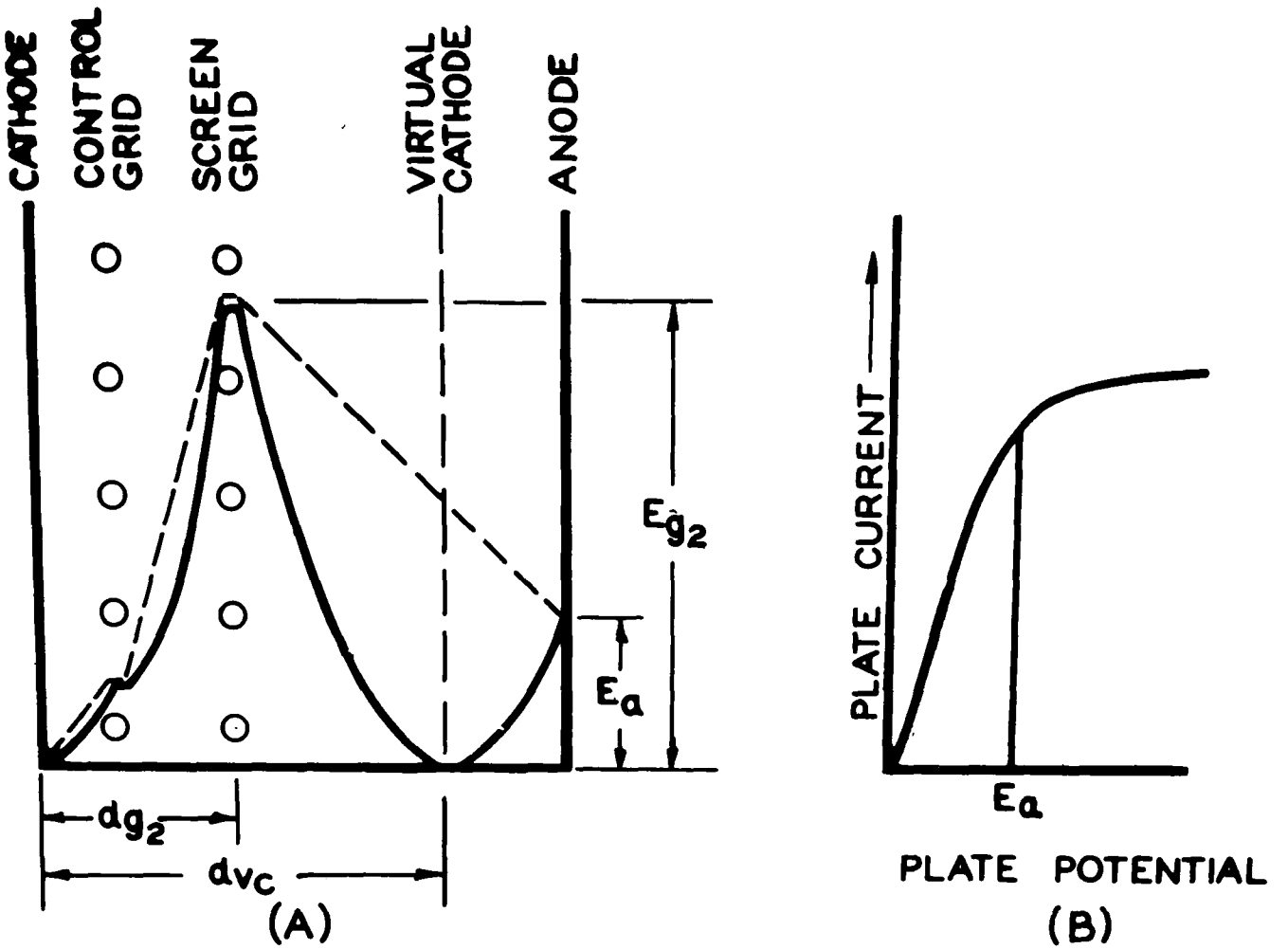

(A) POTENTIAL DISTRIBUTION IN A BEAM TETRODE AT A PLATE POTENTIAL BELOW THE KNEE
(B) AN ILLUSTRATION OF THE OPERATING CONDITION RELATIVE TO THE CHARACTERISTIC CURVE

FIG. 2

In an attempt to verify the theory that the radiation from beam tetrodes resulted from electronic oscillations, the writer developed a relationship for the frequency of the radiation to be expected from beam tetrodes under the assumption that full space charge was present (13). The calculated frequencies had an order-of-magnitude correlation with the measured frequencies; however, the measured radiation covered such a wide band of frequencies that it was impossible to draw a conclusion other than that oscillation of space charge was probably responsible for the radiation. The reason that the radiation from beam tetrodes covers such a broad band is that the potential distribution is highly non-linear and variations in geometry could create several regions which have different oscillation frequencies.

In working to prevent radiation from a sheet-beam frequency demodulator, the writer discovered that tubes of this type produce radiation of a much narrower band than that from "grid-type" tubes normally used as Barkhausen oscillators. The use of a sheet-beam system in which the electrons from the cathode are collimated by a modified Pierce gun affords a means by which radiation of a high spectral purity can be generated, thus permitting better comparisons between theoretical and experimental results.

AN EXPERIMENT TO DETERMINE THE CAUSE OF RADIATION

The lack of tube dimensions in the existing literature prevents use of published information for the purpose of investigating possible oscillation mechanisms other than those proposed by the authors. Furthermore, most of the oscillators were of the wire-grid-accelerator type, usually having cylindrical configurations. In tubes of this type, the potential distributions vary widely as a function of the electron path from the filament to the point of reflection.

The oscillator used in this investigation consists of an electron lens system which is designed to restrict the motion of the electrons to paths over which the potential can be determined accurately. This feature maximizes the accuracy of the transit time calculations. A further reason for the selection of this oscillator configuration, as cited previously, is that the radiated frequency is of a narrower band than that from a would-grid-accelerator design.

Construction of the Experimental Oscillator

Figure 3 shows the configuration and dimensions of the experimental oscillator used in this investigation. The oscillator contains two elongated Pierce guns, one on

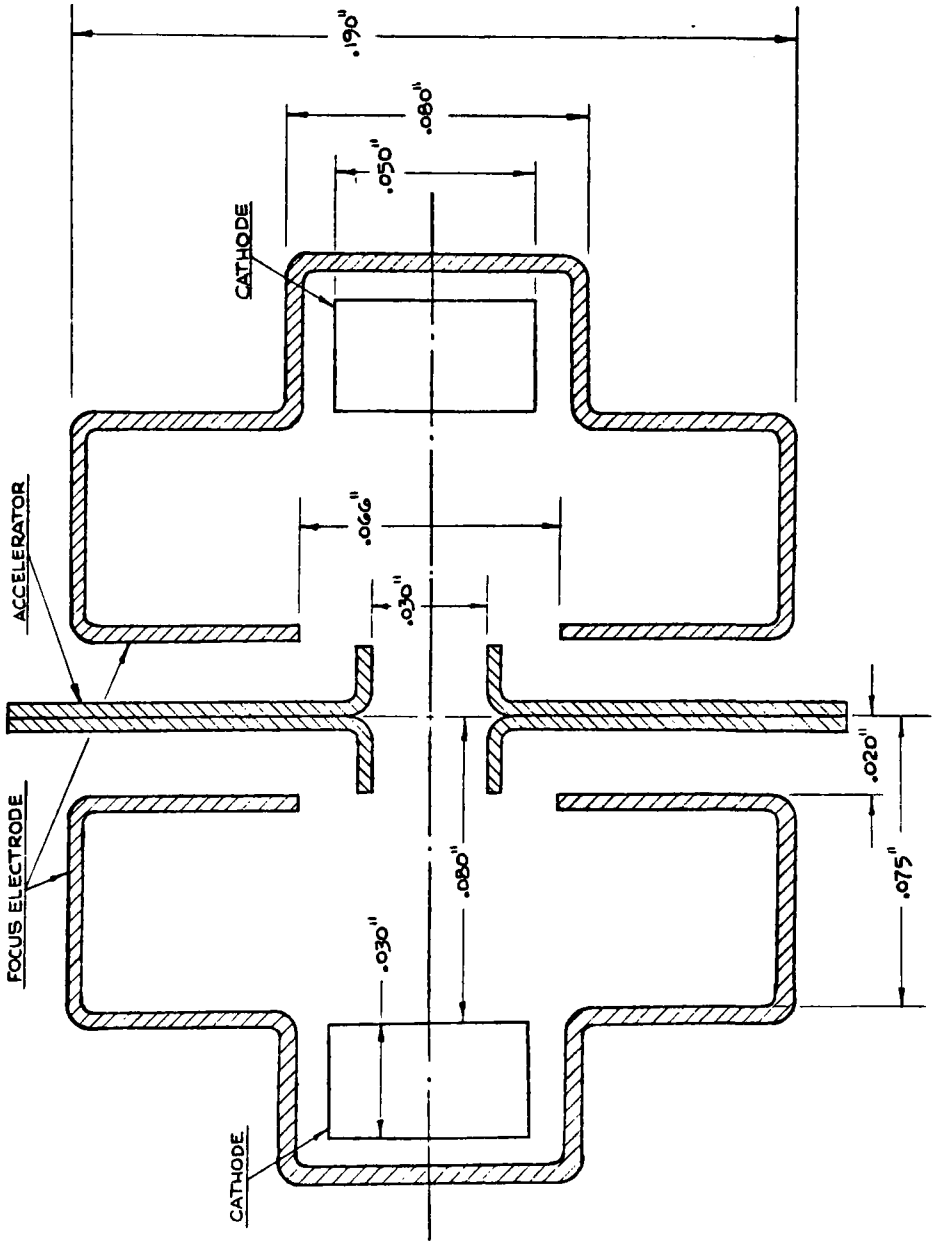

Figure 3. Cross-Section of the Experimental Oscillator.

each side of the accelerator. These guns focus the emitted electrons into beams which are directed through the aperture in the accelerator. Thus the oscillator is symetrical about the plane of the accelerator. Both of the cathodes contain heaters. This arrangement allows current to be drawn from either cathode while the other acts as a reflector, or both cathodes may be operated simultaneously.

The cathode sleeves are made of .0021 - inch-thick, active-alloy cathode nickel. The cathode coating is $BaCO_3$ + $SrCO_3$. All of the other electrodes are made of .005 - inch thick, nickel-plated steel. The parts are spaced and supported by mica insulators. The oscillator is sealed in an 0.80 - inch diameter, 2 - inch-long bulb. Evacuation of the bulb was done with an oil diffusion pump. Pressure in the bulb was first reduced 5×10^{-5} Torr; then the parts were outgassed by inductively heating them to 900° K for three minutes. At this pressure, the temperature of the cathodes was raised to 1200° K for thirty seconds to reduce the Ba and Sr carbonates to oxides. Following activation, the evacuation tube was sealed by melting, and a barium getter film was flashed on the inner surface of the dome of the bulb by inductive heating. The pressure inside the bulb was reduced to approximately 10^{-9} Torr by flashing the getter. The finished oscillator is illustrated in Figure 4.

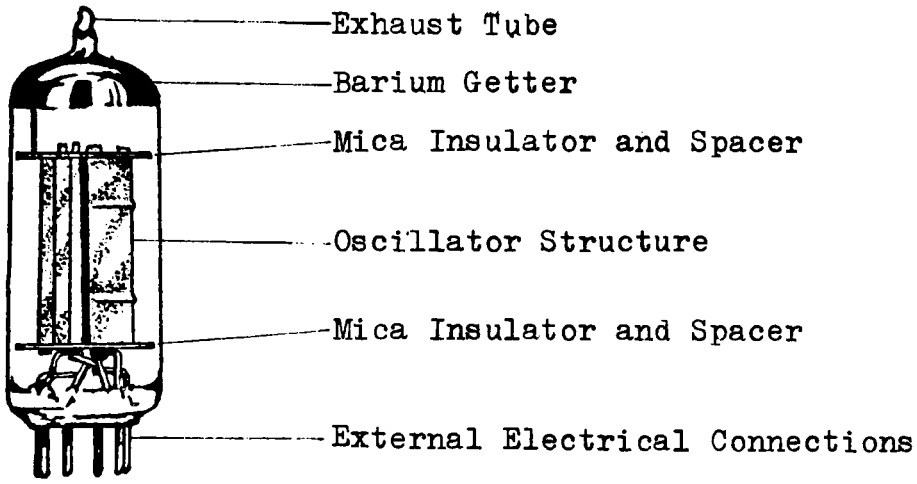

Figure 4. Illustration of the Completed Oscillator.

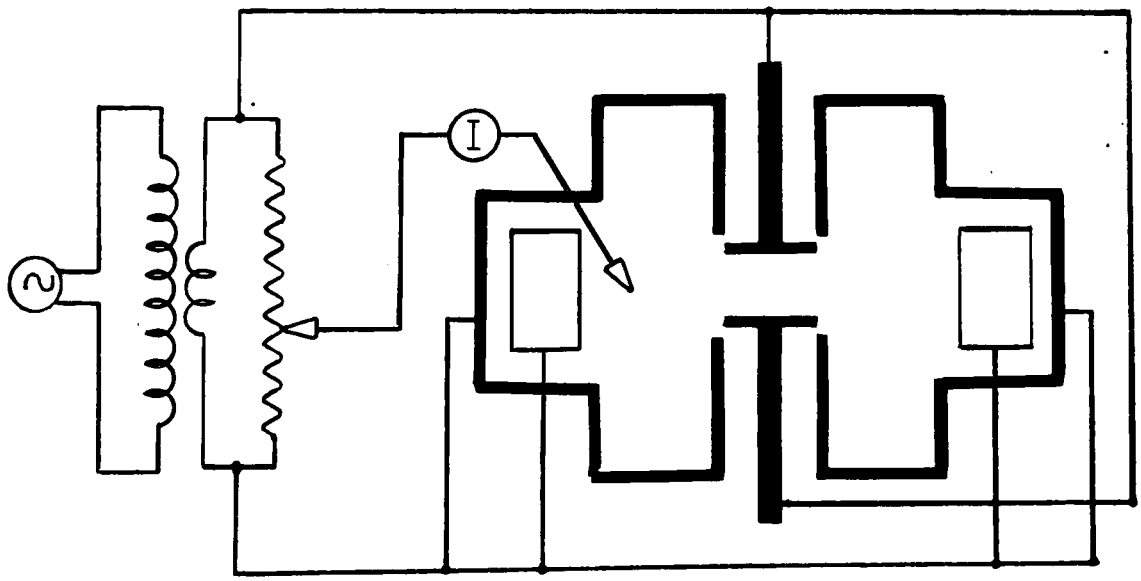

Figure 5. Schematic of Circuit for Determining the Potential Distribution of the Oscillator.

Potential Distribution of the Oscillator

A potential distribution map of the oscillator was made by using a paper having a resistive surface on which a 25:1 scale representation of the oscillator was drawn with electrically conducting silver paint. Potentials were applied to the silver electrodes as shown schematically in Figure 5.

The potential of the accelerator was chosen to be 100 per cent, and all of the other electrodes were connected to the ground terminal. Through use of a ten-turn potentiometer, the potential of the probe could be adjusted in increments of 0.1 per cent from zero to 100 per cent. Assume that the potential of the probe is set at twenty per cent; the galvanometer in the probe circuit will indicate a current until the probe is positioned at a point on the resistive surface at which the potential is twenty per cent. Equipotential lines were generated through use of the one-to-one pantograph in which the probe, mounted in one side, positioned a marker, mounted in the other side, over a scale drawing in proper registry with the conductive-coating drawing. Figure 6 illustrates the potential map obtained by this means. Figure 7 shows the potential distribution along the axis of the beam as determined from the potential map. This graph represents the potential distribution of the oscillator in the absence of space charge.

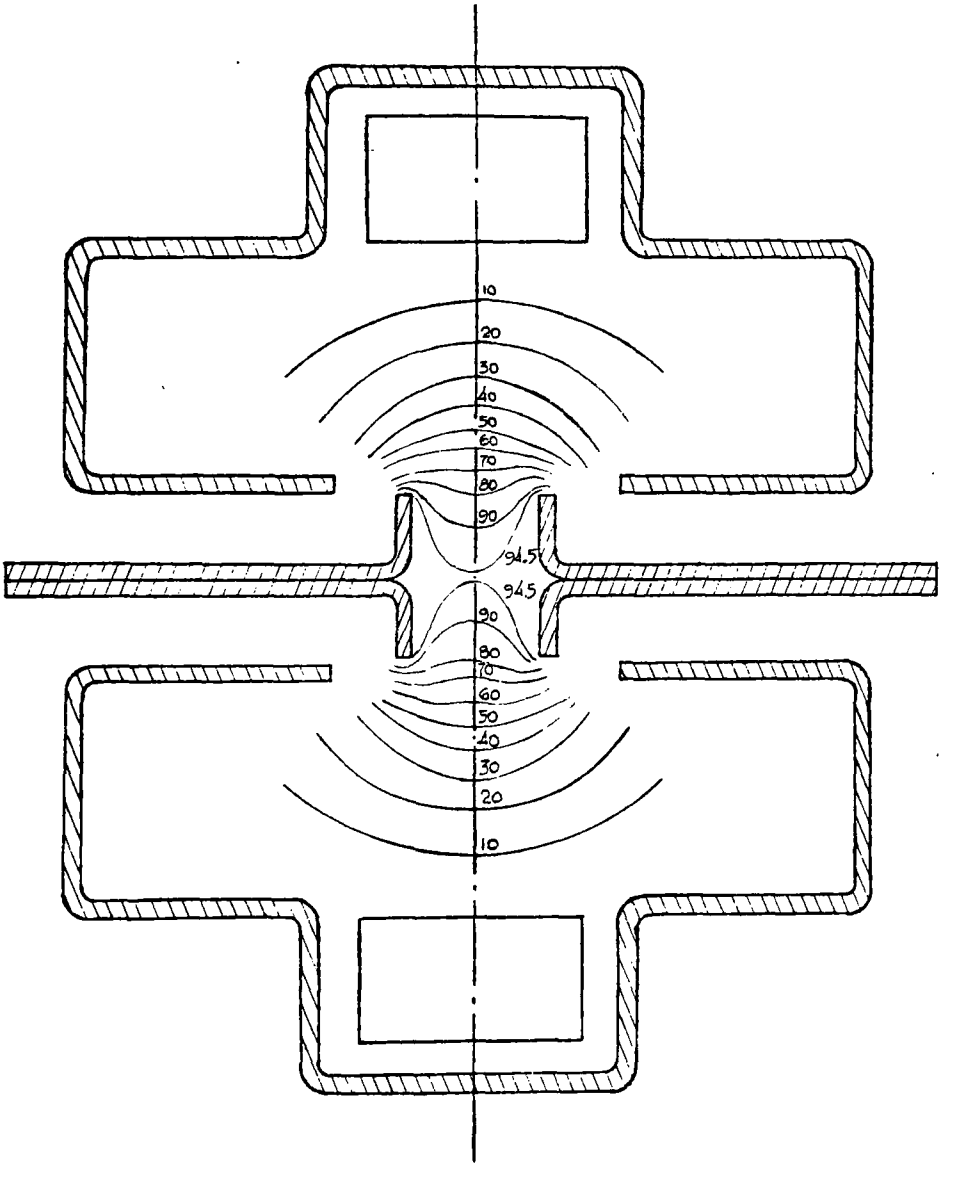

Figure 6. Potential Distribution of the Oscillator.

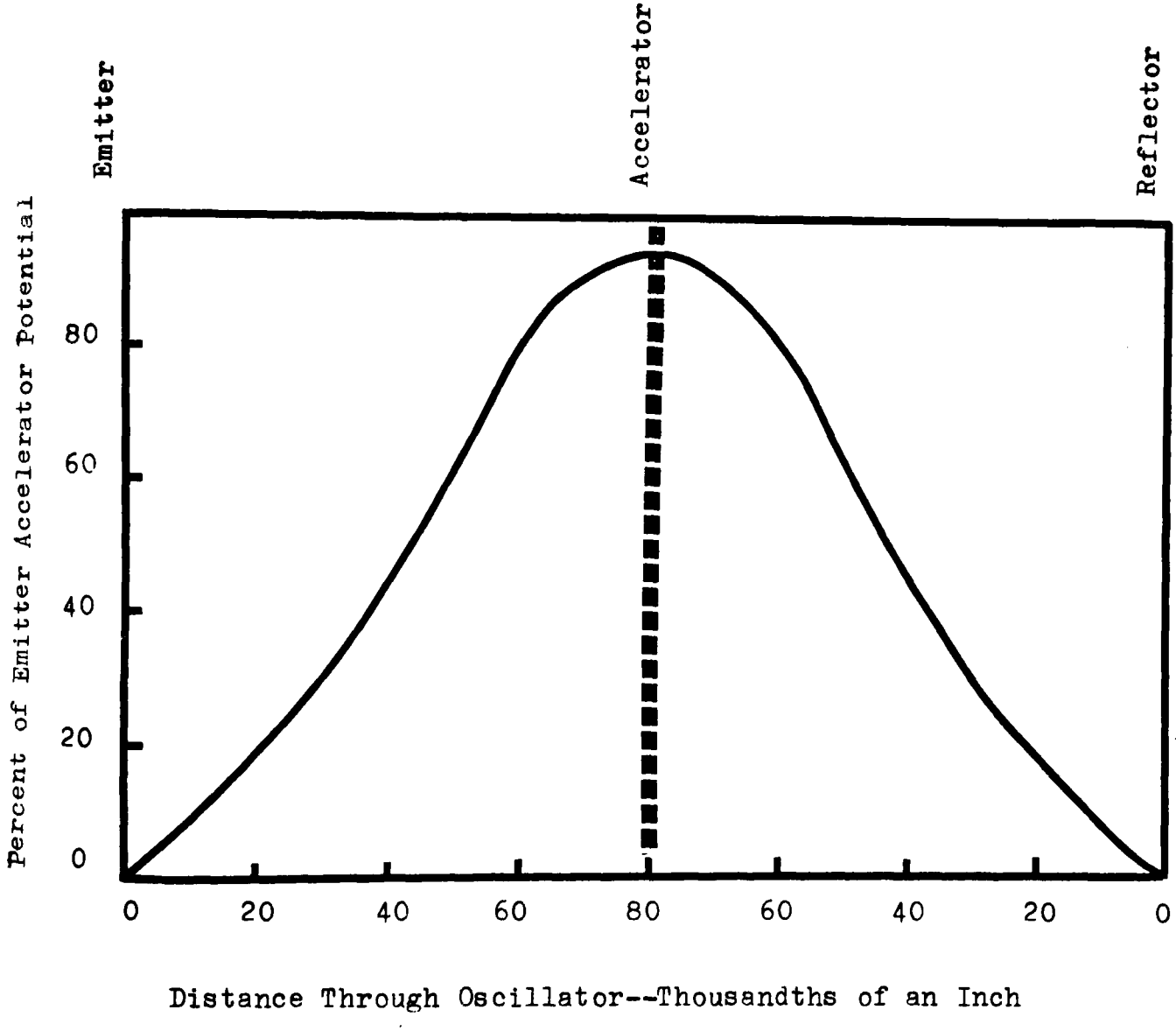

Figure 7. Effective Potential Along the Electron Beam. Transit time was calculated by dividing the path from the emitter to the accelerator into 16 segments and assuming the potential gradient to be linear over that segment.

Measurement of the Radiation

Equipment

Three different receivers were used to detect the radiation from the oscillators.

For frequencies from 174 to 210 MHz and the frequencies of 470 and 536 MHz a VHF-UHF television receiver was used. The frequencies of 210, 470, and 536 MHz could be well established by first tuning the receiver to the commercial broadcast stations broadcating at those frequencies in the area, then moving the antenna to pick up radiation from the oscillator. A UHF receiver for measuring frequencies from 470 MHz to 725 MHz was composed of a calibrated UHF tuner, an IF amplifier and video amplifier.

Frequencies from 100 to 420 MHz were detected on a Navy Department TS - 587/U Noise-Field Intensity meter.

When using both the VHF-UHF television receiver and the calibrated UHF receiver, the presence of the signal was indicated by coupling the output of the video amplifier to modulate the trace intensity of a Tektronix 570 receiving-tube-characteristics, curve-tracing oscilloscope.

The presence of the signal was detected by an audio output to earphones when using the Noise-Field Intensity meter.

A Lambda Model 141 power supply, having a range of 0 to 600 volts, was used to provide an accurate potential source once radiation points were identified on the oscilloscope. The supply was continuously used as a static potential source when detecting radiation with the Noise-Field Intensity meter.

Experimental Procedure

The principal experimental procedure for studying the characteristics of the radiation was a modification of a procedure outlined by L. J. Maginn (14).

The tube was connected to the oscilloscope such that the internal sweep generator would apply a sine-wave potential to the accelerator relative to both cathode-reflector and focus electrodes. In some instances, dc negative potentials, relative to the cathode-reflector electrodes, were applied to the focus electrodes to improve the focus characteristics or to test special effects.

The sine-wave potential applied to the accelerator simultaneously sweeps the oscilloscope trace horizontally across a graduated scale. Vertical deflection of the oscilloscope trace is proportional to the current drawn by the accelerator. The brightness of the oscilloscope trace is modulated by a signal from the video amplifier of the receiver. A brightening of the oscilloscope trace is the indication that the tube is radiating.

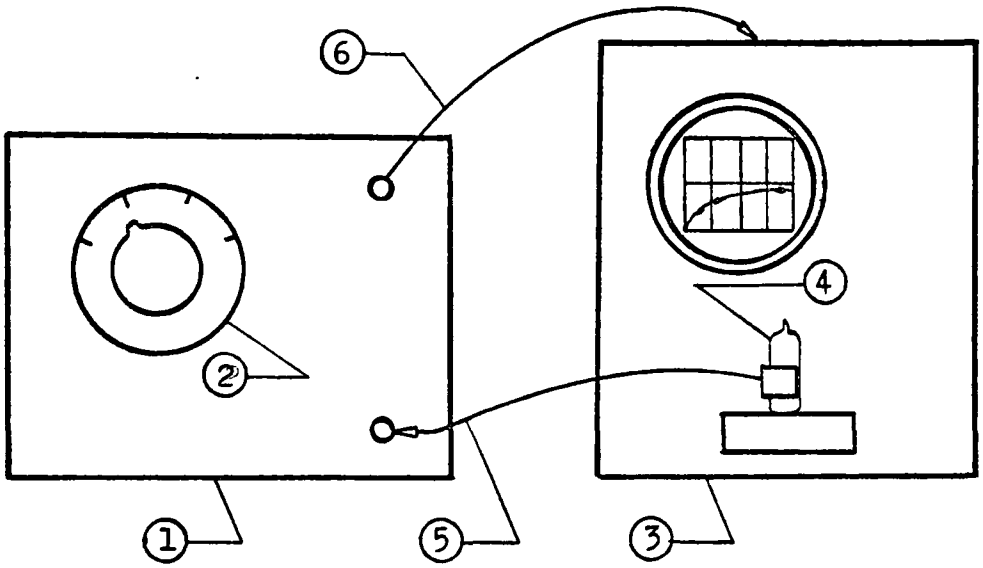

(1) UHF Receiver, (2) Calibrated Tuning, (3) Oscilloscope and Source of Oscillator Driving Voltage, (4) Oscillator, (5) Transmission Line to Receiver, (6) Z-Axis Modulation Signal.

Figure 8 A. Illustration of the Test Equipment.

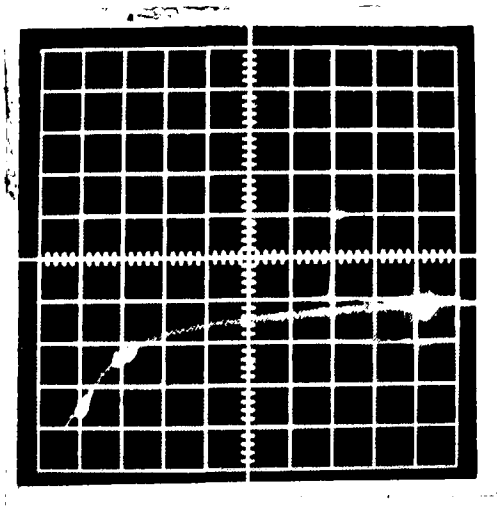

Figure 8 B. Photograph of the Oscilloscope Trace During One of the Test Runs. The receiver was tuned to 470 MHz. The bright spots indicate that the tube oscillates at 470 MHz when the accelerator is at 50, 110, and 460 volts. The horizontal axis is accelerator potential, 50 volts per division. The vertical axis is accelerator current, 50 microamperes per division.

A better understanding and appreciation of the test procedure will be realized by examination of Figure 8A and 8B. Part A of the figure shows the physical arrangement of the tube and test equipment. The tube is held in a socket on the front of the oscilloscope. A slotted cylinder connected to a 600-ohm transmission line couples radiation from the tube to the receiver. The video output from the receiver is fed back to the oscilloscope to modulate the brightness of the oscilloscope trace.

Part B of the figure is a photograph of the oscilloscope display during one of the test runs. The horizontal scale represents fifty volts per division. The vertical scale represents fifty μA of accelerator current per division. The three bright spots on the trace result from the modulation of the oscilloscope beam by the video output of the receiver as a result of radiation emitted by the tube.

Saturation of the current at approximately 200 μA results from the fact that the tube is intentionally being run in the temperature-limited mode to keep the space-charge at a very low level . This eliminates space-charge effects in order to make the potential distribution plots represent a valid model of the tube's potential.

When this photograph was taken, the receiver was tuned to 470 MHz. The tube was being operated with the cathode which is connected to pin number four acting as the emitter. This was accomplished by connecting the

heater of the pin-four cathode to a power source in order to raise the temperature to 400°C. No heater power was applied to the opposite, reflecting cathode. Note that the bright spots show the tube to be radiating a frequency of 470 MHz when its accelerator ia at 50 volts, 110 volts , and 460 volts. The anode potentials were verified by removing the swept voltage from the accelerator and applying a static dc potential from the Lambda power supply. The dc potential was determined by slowly varying the voltage about the points determined by the oscilloscope trace until the receiver output was maximized.

In addition to providing a clear, graphic indication of the radiation characteristics at a given frequency, as illustrated by part B of Figure 8, use of the oscilloscope test method gives a dynamic representation of the radiation effects as the tuner frequency is varied. The bright spots will move to higher voltages when the tuner frequency is increased and to lower voltages as the tuner frequency is decreased.

EXPERIMENTAL RESULTS

Transit-Time Calculations

The potential distribution through the oscillator, represented by Figure 7, was used to calculate the transit time. The potential function was approximated by dividing the path from the cathode to the center of the accelerator into sixteen segments of 1.25×10^{-4} meters and assuming a linear potential gradient over each segment.

Since,

$$\frac{1}{2}mv^2 = eV,$$

then

$$v = \sqrt{\frac{2eV}{m}}$$

gives the velocity, v, of the electron at any potential, V. If V_{n-1} is the potential at the beginning and V_n is the potential at the end of segment n, the average velocity of the electron over that segment will be

$$\frac{v_{n-1} + v_n}{2} = \sqrt{\frac{e}{2m}} \left(\sqrt{V_{n-1}} + \sqrt{V_n} \right).$$

If t_n is defined as the time required for the electron to traverse segment n, then

$$t_n = \frac{\text{segment length}}{\text{average velocity}},$$

or

$$t_n = \frac{d}{\sqrt{\frac{e}{2m}}\left(\sqrt{V_{n-1}} + \sqrt{V_n}\right)}$$

Let τ be the time required for the electron to travel from the cathode to the center of the accelerator. Then τ will be the sum of the transit times of the 16 segments, or

$$\tau = \sum_{n=1}^{16} t_n = \sum_{n=1}^{16} \frac{d}{\sqrt{\frac{e}{2m}}\left(\sqrt{V_{n-1}} + \sqrt{V_n}\right)} .$$

Effects of Accelerator Potential

Table 1 shows the accelerator potential, the observed frequency, the calculated transit time corresponding to the accelerator potential, and the number of transit times represented by the frequency; i. e.,

$$N = \text{Number of Transit Times} = (\tau \cdot \text{frequency})^{-1}$$

Examination of the number of transit times indicated that there are three distributions of N; one about a median of 5.93, one about a median of 2.86 and one about a median of 1.85. These distributions suggest that the radiation being detected could be the fundamental and harmonics as indicated in the following relations:

$$\text{Fundamental Frequency} = (6\tau)^{-1}$$

$$\text{First Harmonic} = (3\tau)^{-1}$$

$$\text{Second Harmonic} = (2\tau)^{-1}$$

To investigate this hypothesis, calculated curves of the fundamental frequency and harmonics as a function

of accelerator potential were plotted along with the data points in Figure 9.

Correlation of the observed and calculated frequencies is seen to be rather good except near an accelerator potential of 200 volts. At this potential, the oscillator would become intermittently unstable and radiate at the frequencies shown on the graph. Attempts to eliminate the instability by introducing chokes and by-pass condensers into the accelerator and reflector circuits were partially successful in reducing the amplitude of the spurious frequencies.

Effects of Current Suppression

In the effort to eliminate radiation from a sheet-beam synchronous detector, it was noted that the oscillation occurred upon initiation of suppression of accelerator current by reflected electrons. Figure 10 illustrates this phenomenon. This figure is a double-exposure photograph of the oscilloscope display of the accelerator current characteristics of the detector section of a 6Z10 audio-detector-amplifier under two conditions of control grid potential.

In the upper curve, the potential of the control grid is above the level at which electrons will be reflected back through the accelerator aperture toward the cathode. The absence of brightness modulation

TABLE I

MEASURED FREQUENCY OF OSCILLATION, CALCULATED TRANSIT TIME, AND NUMBER OF TRANSIT PERIODS FOR CORRESPONDING ACCELERATOR POTENTIALS.

Tube No.	Emitting Cathode	Accelerator Potential (Volts)	Receiver Used	Measured Frequency MHz	Transit Time n Seconds	Number of Transit Times
2	9	580	UHF/VHF	470	.322	6.59
2	9	103	UHF/VHF	210	.765	6.22
2	9	92	UHF/VHF	198	.809	6.23
2	9	81	UHF/VHF	186	.862	6.23
2	9	180	UHF/VHF	536	.578	3.22
2	9	475	UHF/VHF	470	.356	5.97
2	9	130	UHF/VHF	470	.680	3.12
2	9	98	UHF/VHF	192	.784	6.64
2	9	110	UHF/VHF	210	.740	6.43
2	9	80	TS-587	200	.868	5.76
2	9	58	TS-587	155	1.019	6.33
2	9	200	TS-587	382	.549	4.76
2	9	230	TS-587	352	.512	5.55
2	9	190	TS-587	315	.563	5.64
2	9	155	TS-587	275	.624	5.83
2	9	245	TS-587	365	.496	5.52
2	9	180	TS-587	365	.579	4.73
2	9	200	TS-587	335	.549	5.44
2	9	170	TS-587	330	.595	5.09
2	9	322	TS-587	395	.433	5.85
2	4	475	UHF	473	.356	5.93
2	4	45	UHF	473	1.157	1.83
2	4	100	UHF	473	.776	2.72
2	4	50	UHF	500	1.098	1.82
2	4	60	UHF	550	1.002	1.81
2	4	70	UHF	600	.928	1.80
2	4	87	UHF	650	.832	1.85
2	4	90	UHF	725	.818	1.69
2	4	120	UHF	500	.709	2.82
2	4	130	UHF	550	.681	2.67
2	4	155	UHF	600	.624	2.67
2	9	125	UHF	500	.694	2.88
2	9	50	UHF	500	1.098	1.82
2	9	60	UHF	500	1.002	1.99
2	9	119	UHF	700	.712	2.01
2	9	270	UHF	700	.473	3.02
2	9	90	UHF	700	.818	1.75
2	9	60	UHF	575	1.002	1.74
2	9	175	UHF	575	.587	2.96
3	4	105	UHF/VHF	210	.758	6.28

TABLE I--Continued

Tube No.	Emitting Cathode	Accelerator Potential (Volts)	Receiver Used	Measured Frequency MHz	Transit Time n Seconds	Number of Transit Times
3	4	80	UHF/VHF	210	.868	5.49
3	4	65	UHF/VHF	174	.963	5.97
3	4	425	UHF/VHF	470	.376	5.65
3	4	200	UHF/VHF	470	.549	3.88
3	4	50	UHF/VHF	536	1.098	1.70
3	4	92	UHF/VHF	470	.809	2.63
3	4	38	UHF/VHF	470	1.260	1.69
3	4	55	UHF/VHF	470	1.047	2.02
3	4	430	UHF/VHF	470	.374	5.65
1	4	109	UHF	210	.744	6.40
1	4	440	UHF	470	.370	5.75
1	4	50	UHF	470	1.098	1.94
1	4	62	UHF	536	.986	1.89
1	4	60	UHF	540	1.002	1.85
1	4	81	UHF	600	.863	1.93
1	4	119	UHF	700	.712	2.01
1	4	70	UHF	700	.928	1.54
1	4	110	UHF	470	.740	2.86
1	4	145	UHF	550	.645	2.82
1	4	180	UHF	610	.579	2.83
1	4	475	UHF	470	.356	5.93

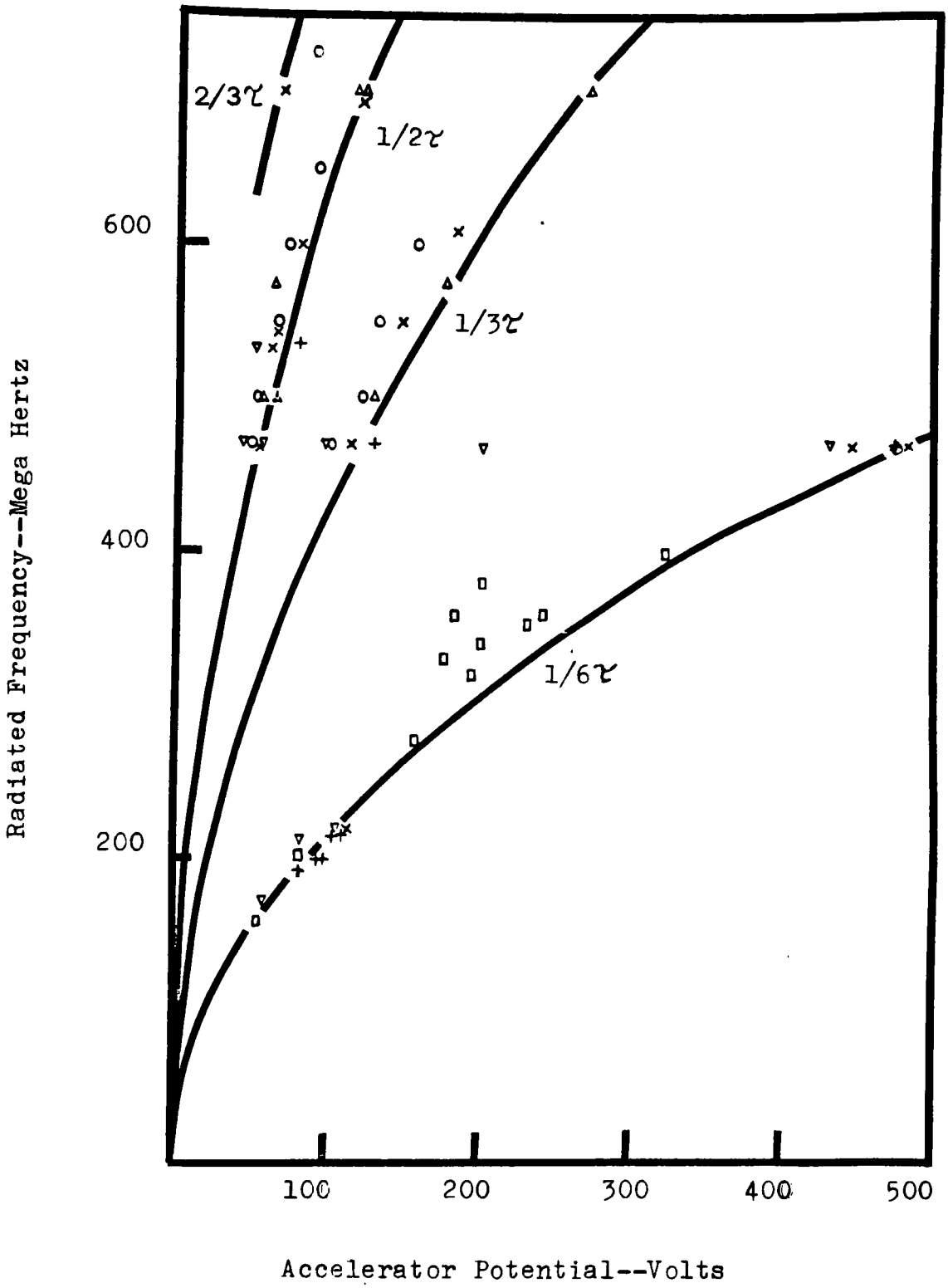

Figure 9. Observed Frequencies and Curves of 1/6γ and Higher Harmonics as a Function of Accelerator Potential.

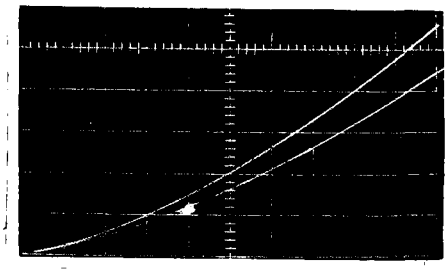

Figure 10. Operating Characteristics of the 6Z10 Before Redesign. Figure 10 is a double-exposure photograph of the oscilloscope trace of a 6Z10 synchronous detector before redesign of the control grid to prevent reflection of electrons through the aperture. The lower trace shows that radiation starts when cathode current is suppressed. The horizontal scale is 20 volts per division, and the vertical scale is 5 mA per division.

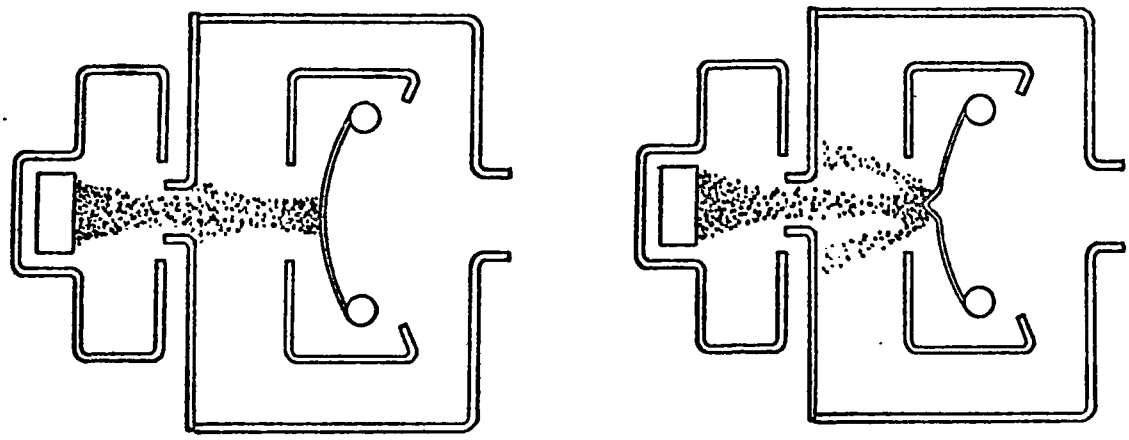

Collimated Reflection

Divergent Reflection

Figure 11. Illustration of the 6Z10 Redesign. Redesign of the control grid to make the reflecting field divergent allowed the control grid to be driven negative without causing the cathode to be suppressed as indicated by the lower trace shown in Figure 10.

of the oscilloscope trace indicates that the tube is not radiating. The receiver, in this instance, was tuned to receive 470 MHz. Upon increasing the bias, two things happened: (1) the accelerator current decreased, as indicated by the lower trace, and (2) the tube radiated at 470 MHz at an accelerator potential of eighty volts as indicated by the brightness modulation. Observation of this effect suggested that the radiation results when electrons are returned to the cathode through the accelerator slot. If this were the case, it should be possible to eliminate the oscillation by redesigning the control grid such that the reflecting field would be divergent and cause the reflected electrons to be directed to the solid portion of the accelerator rather than to the slot and hence back to the cathode.

The control grid was redesigned as shown in Figure 11. The divergent characteristics of the revised control grid are such that increasing the bias on the grid does not cause the accelerator current to be suppressed, and the structure does not radiate (15).

The fact that preventing the return of the electrons to the cathode eliminated the radiation indicated that the oscillation mechanism was some result of electrons returning toward the emitting cathode. Figure 12 shows the current characteristics of the experimental oscillator as a function of reflector potential. Note the

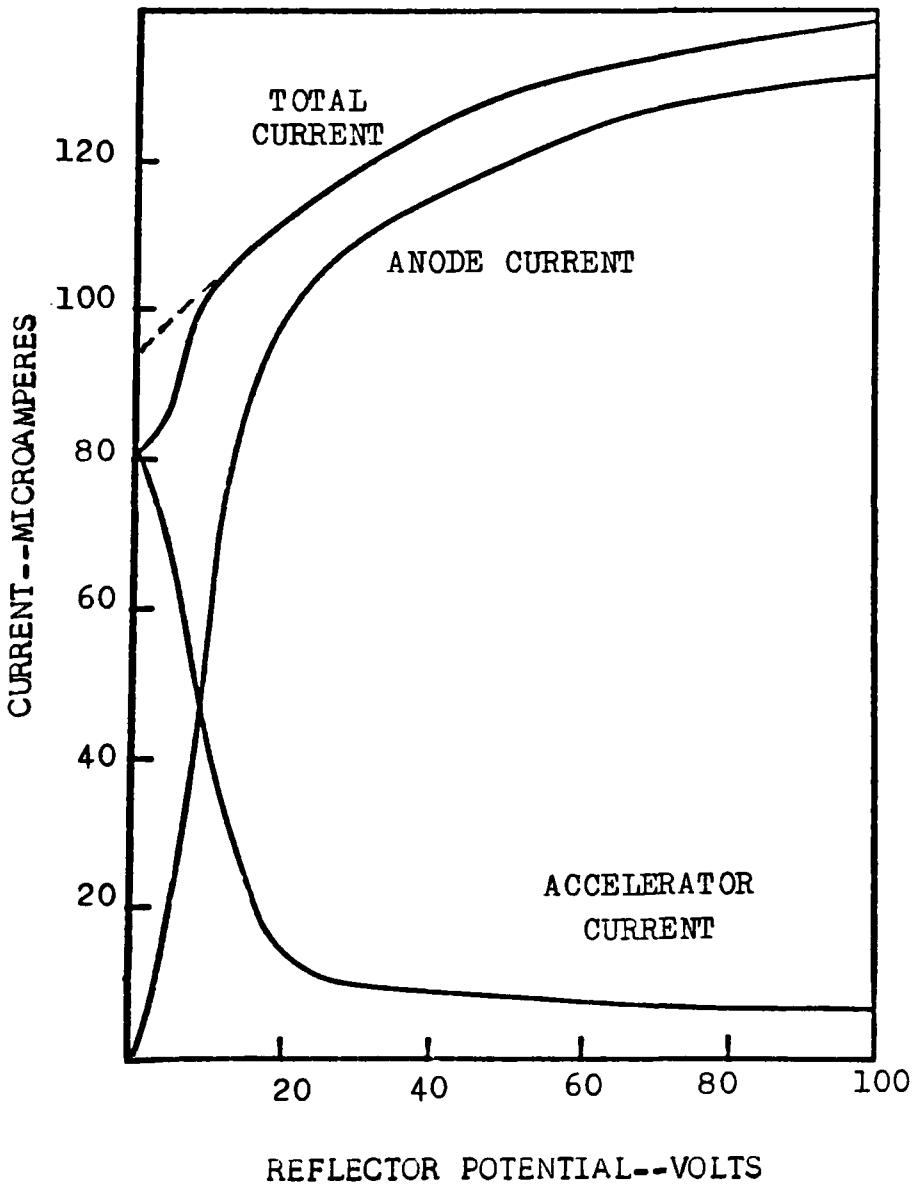

Figure 12. Current Characteristics of the Experimental Oscillator as a Function of Reflector Potential.

sudden decrease in emitting cathode current as the potential of the reflecting electrode is decreased to zero. If the emitting cathode current were a function of equivalent accelerating potential alone, the emitting cathode current should decrease evenly to a level indicated by the projection of the cathode current to the zero-potential axis.

One can assume that the decrease in total current results from the constant reabsorbtion of reflected electrons alone; i. e., the primary emission of current remains essentially constant as determined by Richardson's (18) equation but the steady-state level is reduced by the uniform return of a portion of the electrons. If this were the case, the oscillator could exist in a steady state of equilibrium without radiating.

One can also assume, on the other hand, that the depressed level represents an average current. For example, assume that the returning electrons suppress the primary emission current density. If this were the case, the primary emission current density would vary if the reflected current density varied. Visualize the oscillator if the accelerator potential were suddenly applied at time zero. The primary current density would immediately rise to the level determined by Richardson's equation and remain there for a period until the returning electrons suppress that level. The primary emission level

would then remain low until the current density of the returning electrons decreased following the period required for the electrons of the lower primary emission period to begin returning. If this assumption were true, the returning electrons could cause a pulsation of the emitted current density which would cause the tube to radiate.

This latter assumption is supported by the result that the change in geometry of the control grid of the synchronous detector eliminated both the returning electrons and the radiation by preventing suppression of the emitted current.

Another experimental result which would support the latter assumption would be one in which two cathodes emitting toward each other eliminate the radiation. If two cathodes emit electrons at the same rate, rather than one simply acting as a reflector, it should be possible to "spoil" the pulsation and establish a state of equilibrium in which the primary emission of both cathodes remains constant. If this condition were established, there should be no radiation.

Figure 13 illustrates the results of a test to verify this hypothesis. Part A of the figure is a photograph of the oscilloscope trace when only one cathode is emitting. The peculiar shape of the current characteristics resulted from the focusing action of applying -15 volts, relative to the cathodes, to the focus electrodes to enhance the effect by assuring that both cathodes emitted

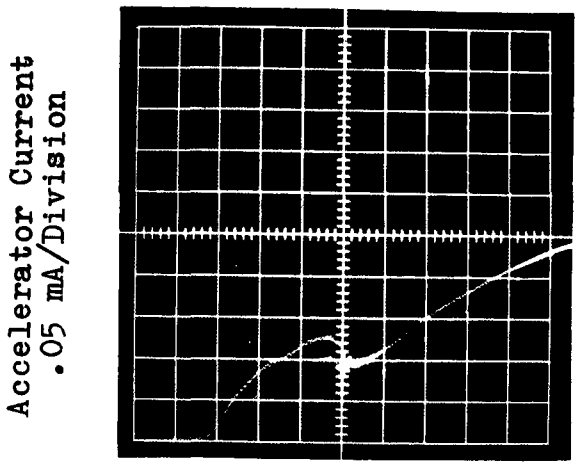

Figure 13A. Photograph of the oscilloscope trace with tube no. 1 being operated with the cathode connected to pin 4 emitting. The radiation indicated at the accelerator potential of 100 volts is 211 MHz.

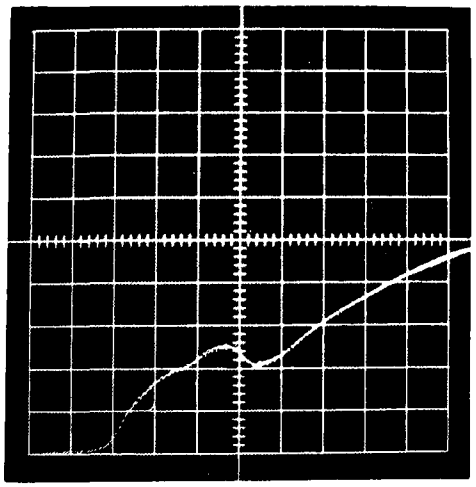

Figure 13B. Photograph of the oscilloscope trace 7 seconds after applying heater power to the reflecting cathode on pin 9. Attenuation of the modulation indicates that the radiation has been suppressed.

Figure 13. Oscillation Suppression by an Emitting Reflector.

toward each other. The focus potential was adjusted such that the detected radiation was positioned in the "trough" of the current trace. The amplitude of the radiation was also intensified by the focusing action. The radiated frequency is 211 MHz at an accelerator potential of 100 volts. After making photograph A, no change was made to the circuit other than to apply power to the heater of the originally reflecting cathode. Initially, there was no change in the trace. As the temperature of the reflecting cathode increased, causing that cathode to begin emitting electrons, the intensity of the radiation continuously decreased. Figure 13 B is a photograph taken approximately seven seconds after power was applied to the second cathode. The attenuation of the radiation is evidenced by the disappearance of the intensity modulation.

Two conclusions can be drawn from the experimental results: (1) The frequency of the radiation appears to be an inverse function of 6γ. (2) The return of reflected electrons toward the emitting cathode is necessary for radiation to occur.

POSSIBLE MECHANISMS OF OSCILLATIONS

There are several established modes in which electronic devices of similar construction generate high-frequency radiation as a result of electronic motion. Each of these types of devices will be examined to determine whether or not the established modes can account for the observed results.

Barkhausen-Kurz and Gill-Morrell Oscillations

Under the assumptions of Barkhausen, the period of oscillation is determined by the time required for an electron to travel from the cathode to the point of reflection and back again to the cathode. Thus the frequency of the Barkhausen model would be $(4\tau)^{-1}$. Although the Barkhausen model does not fit the data in general, a tuned-circuit effect could account for the anomalous readings when the accelerator potential was near 200 volts. For example, Figure 9 shows one data point in which a frequency of 470 MHz was obtained at an accelerator potential of 200 volts. The frequency of this data point is calculated to be $(3.88\tau)^{-1}$.

Gill and Morrell reported that variations in tuned

circuit impedences had a "pulling" effect on the Barkhausen frequency. Figure 9 shows the data to correlate well with the calculated values based on a fundamental frequency of $(6\tau)^{-1}$, except for the region between 150 and 250 accelerator volts where the tube appears to exhibit a double mode of oscillation, one of the Barkhausen-Kurz--Gill-Morrell type and another better characterized by the other data points. The substantial deviation in frequency predicted by the Barkhausen model from the majority of the other data points, however, indicates that those points cannot be accounted for by Barkhausen's theory.

Velocity Variation

The oscillator reported by J. J. Ebers (11) in 1952 was a retarding-field oscillator which utilized a tuned cavity coupled to the accelerator-reflector electrodes. In the Ebers tube, the reflector was designed such that the electrons would be reflected back to the accelerator and not through it. Oscillation was achieved by feedback from the tuned circuit such that the relative potentials of the accelerator and reflector were caused to vary. The relative variation, which was induced by the electron motion, was phased such that the velocity, and hence the depth of penetration into the reflecting cavity, of the electrons would vary and cause electron bunching which would return power to the system to sustain oscillation.

Because of the close similarity of the Ebers tube and the experimental osillator, the velocity-variation mode should be examined to determine whether or not this could explain any of the data points.

Ebers found the fundamental mode to be optimized when the dc transit angle of the electrons was 7.6 radians. In the Ebers analysis, the transit angle is determined by the time that the electron is in the reflecting cavity, which under the system adopted in this paper would correspond to 2γ. This indicates that evidence of velocity-variation effects would be shown by frequencies of $(1.65\gamma)^{-1}$. Examination of the data indicates that there were four readings within $\pm$ ten per cent of this value.

It is difficult to rationalize, however, that the points resulted from velocity variation because the third harmonic of a $(6\gamma)^{-1}$ fundamental would be $(1.5\gamma)^{-1}$, which is also within ten per cent of the velocity-variation frequency. Even if it is assumed that the four points result from the velocity-variation mode, this model is a completely inadequate one for explaining the remaining data points.

Reflex-Klystron Mode

It could be argued that the construction of the experimental tube is similar to that of a reflex klystron and that the focus-electrode-accelerator system functions

in the same manner as do the grids of a klystron in inducing traveling waves on the electron beam.

The mechanism of the klystron is such that oscillations occur at frequencies for which electron transit times are 3/4, 1 3/4, 2 3/4, etc., of the oscillation period. Transit time for the reflex klystron is defined as that period in which the electron is in the reflecting cavity, again corresponding to 2τ. Thus frequencies resulting from klystron action will appear as $(2.65\tau)^{-1}$, $(1.3\tau)^{-1}$, or $(.73\tau)^{-1}$. The data indicate that none of the readings were created by klystron action.

Space-Charge Waves

Space-charge waves can develop when two streams of electrons having different velocities are mixed. In usual devices the two streams that are mixed are traveling in the same direction. Charge concentrations develop and move along with the stream drift. For two electron streams having the same absolute velocity but traveling in opposite directions, there is a condition under which an accumulation of charge builds up but remains stationary. The charge accumulation can create large fields which will eventually reflect the incident streams, causing the charge concentration to dissipate only to build up again as the intermingling of the two streams resumes.

The condition required for charge buildup to

develop in two oppositely directed intermingling streams of the same velocity is

$$0 < \frac{\omega_p}{v} < \sqrt{2}$$

where ω_p is the plasma frequency of the stream in radians per second, and v is the absolute stream velocity in meters per second. The minimum value of the ratio will occur at the highest potential used in the test. At an accelerator potential of 450 volts and a plasma frequency calculated for the center of the accelerator slot, the ratio has a value of sixteen. This indicates that none of the points recorded could have been generated by space-charge waves.

Diode Inertial Effects

One might rationalize that the cathode-accelerator portion of the experimental tube is quite similar to a temperature-limited diode; therefore, this part of the tube could conceivably oscillate in the same manner as a conventional diode can be made to oscillate.

Llewellyn (9) showed that a temperature-limited diode can be represented by an equivalent circuit consisting of a resistance and capacitance in parallel. The dynamic conductance and susceptance of the resistor and capacitance are functions of the frequency of an alternating potential impressed in series with a constant potential across the diode. The diode may be used

as an oscillator at frequencies for which its electronic conductance becomes negative. This conductance becomes negative for electron transit angles between 2π and 2.8π. Therefore, diode type oscillations which might be generated and sustained by some signal mechanism resulting from the reflected electrons would appear as frequencies between $(\tau)^{-1}$ and $(.715\tau)^{-1}$. The readings show that none of the observations resulted from diode oscillations.

A NEW MODEL TO ACCOUNT FOR THE OSCILLATIONS

The analysis in the previous section concerns devices in which the inertial and inductive effects of electronic motion interact with the impedances of the circuit (or with the electron streams themselves in the case of the space-charge wave) to create an oscillation. None of these mechanisms offer satisfactory explanations for the observed results. These failures suggest that a more basic mode of oscillation which is independent of circuit impedances should be sought.

Emission Suppression Model, Temperature Limited

The experimental results indicate that the suppression of electron emission plays an important role in the type of oscillation being observed.

Consider the elementary image-charge model of the surface-potential barrier problem. The effective barrier for an escaping electron would be increased substantially if a returning electron were to approach it. For example, visualize the situation where

an electron which barely has enough energy to overcome the potential barrier is in its lowest kinetic energy state at the barrier peak. Let this electron now be approached by a returning electron which has a high energy relative to the barrier. The approaching electron will prevent the escape of the low energy electron and will itself be absorbed by the cathode. Thus, this very simple thought experiment can serve as the argument for the suppression of primary emission by reflected electrons and can be examined as a model to account for the observed results.

A problem arises, however, after considering that the frequencies of the oscillations are functions of $(6\gamma)^{-1}$. To cause the described effect in the midst of many electrons which are in the cathode-accelerator space, the returning electron would have to be very near the cathode at the time of suppression. If the returning electron were thought of as being a peak in primary emission which had been previously emitted and is now creating a minimum of primary emission, the period between the peak and the minimum of primary emission would be 4γ, and the total period of the cyclic disturbance would be 8γ.

To make the model fit the results, one must assume that suppression does not begin on the approach of the returning electrons to the cathode but instead upon their return through the accelerator slot into the cathode-accelerator region.

Induced Currents

Assume a temperature limited diode in a lossless circuit. An electron emitted from the cathode will gain energy at a rate determined by the product of the force and velocity components,

$$-e\mathcal{E}v.$$

For a parallel plane diode in the absence of space charge

$$\mathcal{E} = \frac{-E}{d}$$

where E is the potential difference in volts between the anode and cathode and d is the separation in meters. Considering only one electron in the space, the power absorbed by the electron can also be represented by the current (i) corresponding to the electron's motion and the potential across the space; so

$$iE = \frac{eEv}{d} .$$

Therefore,

$$i = \frac{ev}{d} \quad ,$$

which expresses Ramo's theorem (16). Thus, during the time that the electron is in transit across the diode, a triangular pulse of current flows in the circuit.

If electrons are emitted at a rate of N per second at the cathode, the total charge that will be emitted during the period t_o to t_o+dt_o will be Ndt_o. The current which will be induced by the charge will then be

$$i = \frac{ev}{d} Ndt_o = \frac{eN}{d} \frac{dx}{dt} dt_o \quad .$$

For a continuous emission of charge, the induced current at any time t will be the sum of all of the contributions of the electrons in the interelectrode space. The electrons contributing to the induced current are those arriving at the anode at time t and all of those emitted in the period $t - \tau$; or

$$i = \frac{eN}{d} \int_{t_o=t-\tau}^{t_o=t} \frac{dx}{dt} \, dt_o \quad .$$

Here, the current at time t is that resulting from emission

at t_o; therefore t is constant and t_o is the variable. Assuming a constant field,

$$\frac{dx}{dt} = \frac{eE}{md} (t-t_o),$$

Therefore,

$$i\ (t) = \frac{e^2 NE}{md^2} \int_{t_o=t-\tau}^{t_o=t} (t-t_o)\ dt_o$$

$$i\ (t) = \frac{e^2 NE}{2\ md^2} \tau^2$$

gives the steady state current induced in the circuit as a result of the summed motion of all of the charges.

Convective Currents

The volume density of traveling-wave states in a crystal is given by (17)

$$\left(\frac{2}{h^3}\right)\ dp_x\ dp_y\ dp_z\ ,$$

where h is Plank's constant, and p is the momentum of the electron. The fraction of these states that will be occupied will be determined by the Fermi function, f (E), which can be approximated by

$$f(E)\ \exp -\left[\frac{E - Ef}{kT}\right] = \exp - \left[\frac{p_x^{\,2} + p_y^{\,2} + p_z^{\,2} - 2mE_f}{2mkT}\right]$$

where Ef is the Fermi energy and k is Boltzmann's constant.

Define a phase-space density function n(r,p) such that

$$n(r,p) = \frac{dn}{drdp} ,$$

where dn is the number of particles in the space dr = dxdydz having momenta in the range of $dp=dp_x dp_y dp_z$. Thus

$$n(r,p) = \left(\frac{2}{h^3}\right) \exp - \left[\frac{p_x^2 + p_y^2 + p_z^2 - 2mE_f}{2mkT}\right]$$

The current per unit area that will be emitted by the cathode will result from the product of the x-directed velocity and number of electrons which have x-directed momenta sufficient to overcome the work function, E_ϕ , of the cathode; or

$$J = e\int_{p_y=-\infty}^{\infty}\int_{p_z=-\infty}^{\infty}\int_{p_x=\sqrt{2mE_c}}^{\infty} v_x n(r,p)dp ,$$

where Ec is the critical energy for the electron to escape. Thus

$$J = \frac{2e}{mh^3}\int_{-\infty}^{\infty}\exp-\left[\frac{p_y^2}{2mkT}\right]dp_y \int_{-\infty}^{\infty}\exp-\left[\frac{p_z^2}{2mkT}\right]dp_z \int_{\sqrt{2mE_c}}^{\infty}\exp-\left[\frac{p_x^2-2mE_f}{2mkT}\right] p_x dp_x$$

$$= \left(\frac{4\pi mek^2}{h^3}\right)T^2 \exp-\left[\frac{E_c - E_f}{kT}\right] ,$$

where (Ec-Ef) is the work function of the cathode. The resulting equation is the well-known Richardson-Dushman relation. Thus the emitted current results from a drift of electrons having energies greater than the critical energy to overcome the potential barrier. Just outside the emitter surface, then, the density function becomes,

$$n(r_o,p) = \frac{2}{h^3} \exp-\left[\frac{p_{x_o}^2 + p_{y_o}^2 + p_{z_o}^2 - 2mE_\phi}{2mkT}\right].$$

Or, in terms of velocity space, the density function becomes

$$n(r_o,v) = 2\left(\frac{m}{h}\right)^3 \exp\left[\frac{-E_\phi}{kT}\right] \exp-\left[\frac{m}{2kT}\ (v_{x_o}^2 + v_{y_o}^2 + v_{z_o}^2)\right]$$

at the surface of the cathode (18). The volume density of the electrons at the surface of the temperature-limited cathode is given by

$$n_t = \int_{-\infty}^{\infty} dv_y \int_{-\infty}^{\infty} dv_z \int_o^{\infty} n(r_o,v)\,dv_x = \left(\frac{2\pi mkt}{h^2}\right)^{3/2} \exp\left[\frac{-E_\phi}{kT}\right].$$

Under temperature-limited conditions, this relation describes the density when all electrons are being removed by the field; none return. Substitution of n_t in the general relation gives

$$n(v_o v) = 2n_t \frac{m}{2\pi kT} \exp-\left[\frac{m}{2kT}\ (v_{x_o}^2 + v_{y_o}^2 + v_{z_o}^2)\right]$$

In the case of a one dimensional field, represented by a parallel-plane diode and to a close approximation by the oscillator, the lack of a potential gradient in the y and z directions results in unchanging velocities in those directions after emission; i. e.,

$$v_y = v_{y_o} = \text{a constant}$$

$$v_z = v_{z_o} = \text{a constant}$$

for all values of x. Along the x dimension, however,

$$v_{x_o} = v_x - \sqrt{\frac{2eE}{m}} = \text{a constant}$$

where E is the potential at point x relative to the cathode.

Thus, the general phase-space density function external to the cathode becomes

$$n(r,v) = 2n_t \left(\frac{m}{2\pi kT}\right)^{3/2} \exp\left[\frac{eE}{kT}\right] \exp -\left[\frac{m}{2kT}(v_x^2+v_y^2+v_z^2)\right]$$

The form of the density function is substantially simplified by making the substitutions

$$\frac{eE}{kT} = \eta - \eta_o \quad ;$$

$$\frac{m}{2kT} v_x^2 = w_x^2;$$

$$\frac{m}{2kT} v_y^2 = w_y^2;$$

$$\frac{m}{2kT} v_z^2 = w_z^2 .$$

Since

$$dN = n(r,v)\ drdv = n(r,w)\ drdw;$$

then

$$n(r,v) = n\ (r,w)\ \frac{dw}{dv} = n(r,w)\ \left(\frac{m}{2kT}\right)^{3/2};$$

therefore,

$$n(r,w) = n_t\ 2\pi^{-3/2}\ \exp\ (\eta - \eta_o)\ \exp\ -(w_x^2+w_y^2+w_z^2).$$

Lindsay's (18) use of this density function helps to simplify the analysis of thermionic emission.

The current density as a function of distance along the path from cathode to anode is given by

$$J(r) = \int v\ n\ (r,v)\ dv$$

$$= \left(2kT\right)^{1/2} \int w\ n(r,w)\ dw$$

$$= n_t\ 2\pi^{-\frac{1}{2}} \left(\frac{2kT}{m}\right)^{\frac{1}{2}}\ \exp\ (\eta - \eta_o) \int_{\eta^{\frac{1}{2}}}^{\infty} w_x\ \exp(-w_x^2) dw_x$$

$$= n_t\ 2\pi^{-\frac{1}{2}} \left(\frac{2kT}{m}\right)^{\frac{1}{2}}\ \exp\ (\eta - \eta_o)\ \ \exp\ (-\eta)$$

$$= n_t\ \left(\frac{2kT}{m}\right)^{\frac{1}{2}}\ \ \exp\ (-\eta_o).$$

In a temperature-limited diode, η_o represents the cathode surface potential, which is constant. Therefore, the convection current density of a parallel plane diode

is independent of x.

Thus, in the steady-state condition, the emission current density at the surface of the cathode is constant and independent of time; the current density at any plane perpendicular to the direction of flow is constant throughout the space between electrodes; and, from the previous section, the induced current is independent of time and is the sum of the contributions of all of the electrons in the interelectrode space.

Effects of Electron Drift

Within the emitter, there must be a net drift of electrons, having sufficient energy to escape, moving toward the surface. Thus, at the surface,

$$n(r,w) = n_t \, 2\,\pi^{-3/2} \exp -(w_x^2+w_y^2+w_z^2)$$

can be integrated to give the volume density when no electrons are returned to the cathode by integrating with respect to w_y and w_z between the limits of $\pm\infty$ and with respect to w_x over the limits 0 to ∞, resulting in

$$n(r_o) = n_t .$$

If, however, the electrons were immediately reflected at the surface, wx would be integrated over

the limits $-\infty$ to $+\infty$, resulting in

$$n(r_o) = 2\, n_t \ .$$

Visualize a situation in which the electrons are immediately reflected at the surface. Just inside the surface the densities of electrons and their velocity distributions are identical to those of an emitter in thermodynamic equilibrium: there is no net drift. Immediate dissolution of the reflecting plane at the surface would allow the high energy electrons to escape, causing a flow of electrons toward the surface.

Figures 14 A and B illustrate the effects of electron emission at a surface. Figure 14 A illustrates the electron density in the body of an emitter where there is no net current flow. (19) Figure 14 A can also be used to illustrate the electron density at the surface of an emitter where there is an infinite potential barrier at the surface: the electrons approaching the barrier by traveling in the positive x direction are reflected by the barrier and continue to travel at their previous energy level but in the negative x direction. Figure 14 B illustrates the electron densities at the surface of the emitter when the infinite barrier has been removed, permiting electrons to escape and creating an induced flow of electrons to the surface as a result of the escape of the energetic electrons.

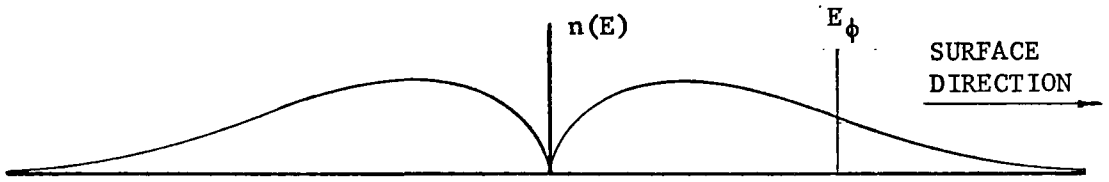

A) Energy Distribution in a Semiconductor Emitter When there is no Current Flow.

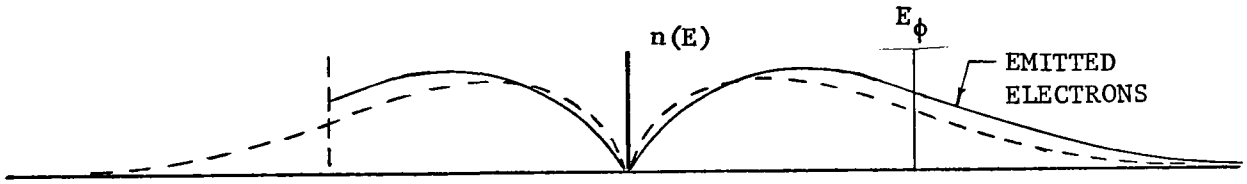

B) Energy Distribution at the Surface of a Semiconductor During Temperature-limited Emission. The dotted line is a repeat of A), above, for reference. On the right, the solid line indicates a shift of the electrons to higher energy levels as a result of flow toward the surface. Note that the shift increases the number of electrons having escape energies. The solid line on the left illustrates reflection of the lower energy electrons by the barrier.

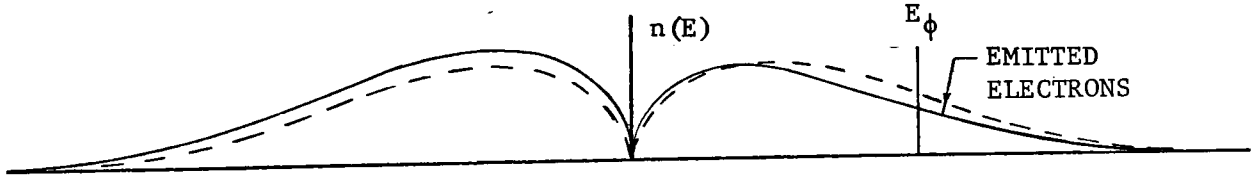

C) Electron Energy Distribution when Previously Emitted Electrons, are Being Returned. Note that the induced flow decreases the number of electrons having escape energy. A), dotted, is again repeated for reference.

Figure 14. Electron Energy Distributions in the Emitter

The effect of the flow is to shift the electron densities to higher energy levels in the positive x direction and to lower levels in the negative x direction. The effect is that the effective Fermi level in the positive x direction is shifted toward the work-function level, increasing the number of electrons having escape energy relative to the number which have energies exceeding the work-function energy in equilibrium. One can use this model to rationalize that the emitted current in the case where no electrons are being returned would be higher than that being emitted when electrons are returning.

In the previous derivation of the Richardson-Dushman equation, the model illustrated by Figure 14 A is assumed. The temperature-limited density of electrons just outside the surface, n_t, results from those electrons having energies exceeding E_ϕ. The result that $n(r_o) = 2n_t$ when electrons are totally reflected is also based on the model illustrated by Figure 14 A. Using the same model illustrated by both cases is incompatible for in the former case there is a net flow of electrons in the emitter and in the latter there is none. Inasmuch as the number of electrons in the higher levels decreases rapidly as a result of the Fermi function, the error introduced by neglecting

the shift is small such that the observed results with conventional applications have been relatively well predicted by the theory.

It was previously shown that the current density in a parallel-plane diode, or in the cathode accelerator region of the oscillator, under steady-state conditions is independent of both distance and time. Figures 15 A and B illustrate the electron flow in an idealized oscillator which is assumed to have an accelerator which can be made opaque or perfectly transparent to electrons for the situation based on the Richardson-Dushmann mode when no electrons are returned and when all electrons are returned, respectively. Two incompatibilities become evident: 1) As previously cited, the electron flow outside the emitter as shown by Figure 15 A is not compatible with the situation inside the emitter illustrated by Figure 14A. 2) Figure 15 B illustrates a highly idealized situation which is unattainable in practical situations; i. e., total reflection will double the space charge and the potential gradient at the emitter will be decreased such that the magnitude of the primary emission will be reduced on the basis of the Schottky effect.

Now assume that the model illustrated by Figure 14 B is correct such that the flow of electrons to an

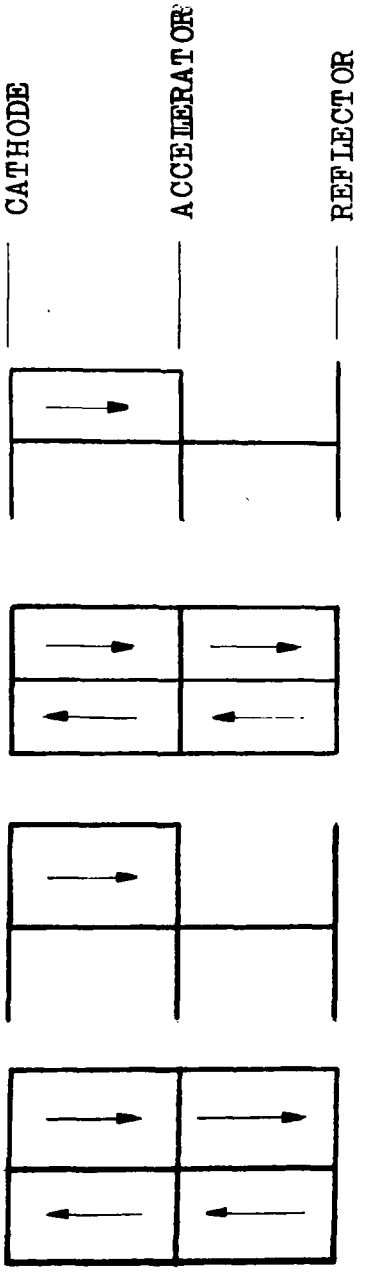

Figure 15 A. Opaque accelerator and current determined by the Richardson-Dushman relation.

Figure 15 B. Transparent accelerator and emitted current determined by Richardson-Dushman relation.

Figure 15 C. Opaque accelerator and current determined by the Richardson-Dushman relation increased by drift effects.

Figure 15 D. Transparent accelerator with increased emitted current.

Figure 15. Convective Current Flow Diagrams with Reflections.

opaque accelerator will be higher than that predicted by the Richardson-Dushman relation. In this case, the flow to the accelerator is shown in Figure 15 C, and the model for the flow inside the emitter is compatible with the flow outside the emitter. If the accelerator is now made transparent, Figure 15 D illustrates a situation, again, which cannot exist. The closest model that could be used for the steady-state of Figure 15 D would be the equilibrium model of Figure 14 A. However, the levels of the returning electron current at time $t = 4\tau$ would have to be that shown in the cathode-accelerator region of Figure 15 C. The returning current would exceed that being emitted, which would serve to decrease the emitted current to a level below that predicted by the Richardson-Dushman relation.

The conclusion that can be drawn from the foregoing is that a thermionic cathode emitting into a potential well in which there is a finite time between emission and return of the electrons cannot establish a state of equilibrium. The reason equilibrium cannot be established is that the emitted electron current is affected by the returning electron current which was emitted at a previous time.

The problem is to find a model in which the electron flow within the emitter and that in the cathode-accelerator region are compatible. Since all circuit impedances are being purposely ignored, all electrode potentials will be considered to remain constant. It is further assumed that the plane of the accelerator effectively shields the electronic motion in the reflecting cavity from the cathode-accelerator space. Therefore, it is only necessary that flow compatibility exist in the cathode-accelerator region.

The induced current density must result from the vector sum of the motions of all of the electrons in the cathode-accelerator space. The instantaneous emitted and reflected currents will vary; therefore the instantaneous convective current will vary as a function of time. If the convective current were represented, as was done in Figure 15, on a distance base, the time varying function will become distorted in its representation as a result of acceleration of the beam. This distortion can be eliminated by representing the current on a time, rather than distance, base. The induced current density can be expressed in terms of convective currents by the relation

$$J = \frac{\rho_1 v_1 \Delta t_1}{\tau} + \frac{\rho_2 v_2 \Delta t_2}{\tau} + \cdots \frac{\rho_n v_n \Delta t_n}{\tau} ,$$

where $\rho_n v_n$ is the particular convective current density flowing during a period Δt_n. Here v is the vector velocity of the current density, the convention being chosen that electron flow from the emitter toward the accelerator is positive .

Starting with a diagram of the type illustrated by Figure 15, but on a time base, one can make continuous iterations, adjusting the emitted current density to account for suppression by returning electrons, and arrive at the diagram shown in Figure 16.

Figure 16 illustrates the convective current density at a series of times τ seconds apart. Consider the first portion of Figure 16 representing the situation at t = 0. The emitted current density is at a maximum. It is assumed that the accelerator is perfectly transparent such that all electrons emitted are eventually returned. At t = 0, the reflected current is at its lowest level at the plane of the accelerator. The difference between the instantaneous convective current at the accelerator and the median level designated by the dotted line is equal to the difference at the emitter. The magnitudes of the convective currents at the reflecting plane are equal but opposite in direction.

At t = τ, the positive maximum has moved to the center of the accelerator slot. The emitted current is

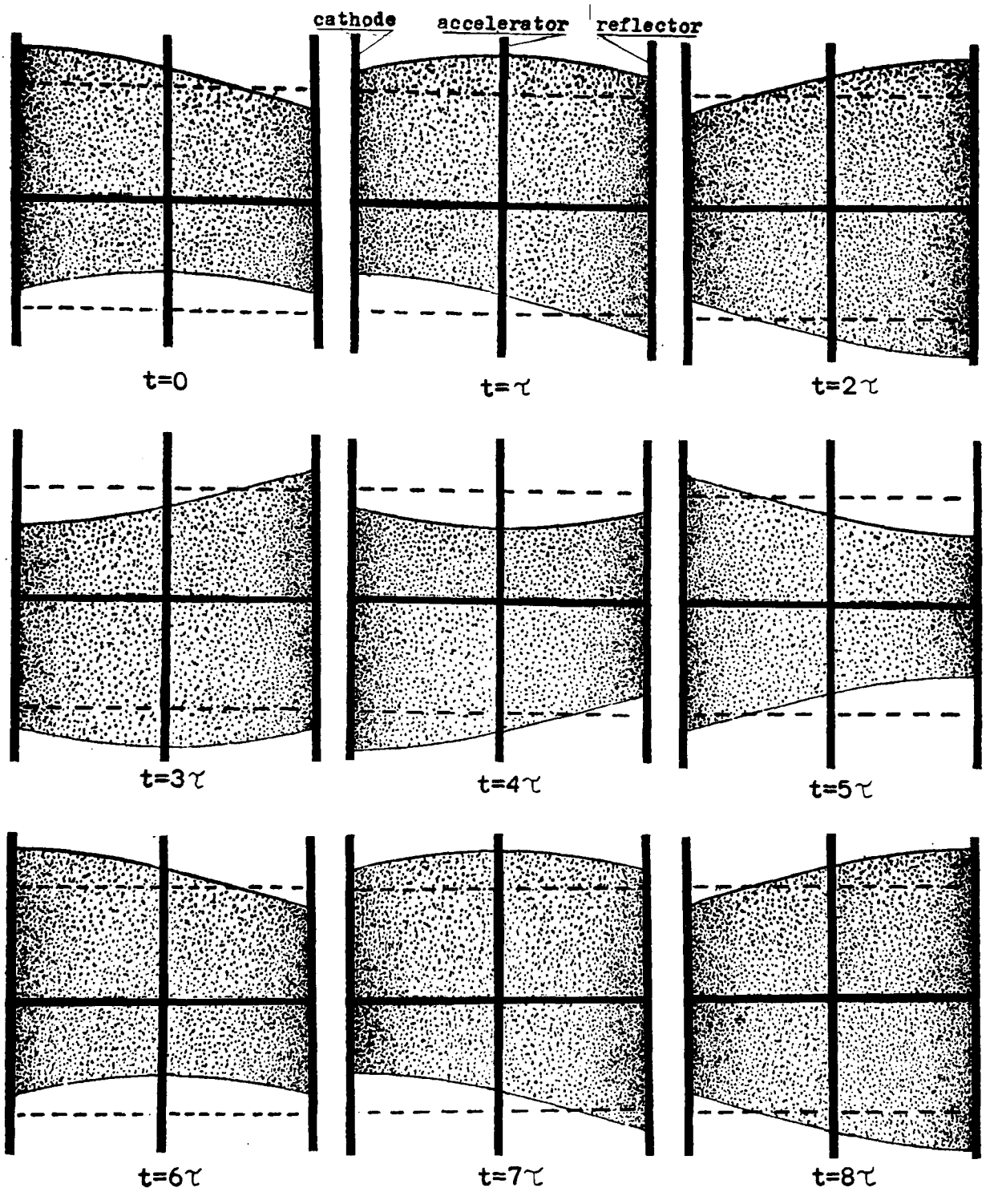

Figure 16. Convective Current Densities on a Time Base. The plots above the horizontal axis represent electron flow away from the cathode. Plots below the horizontal axis represent electron flow toward the cathode.

decreased by the amount that the reflected current has increased at the plane of the accelerator. Again, the positive and negative current magnitudes at the reflector are equal. It can be seen that the pattern is the same in each of the subsequent figures.

Several significant factors are demonstrated by Figure 16:

1) The cycle repeats in a period of 6τ.

2) The absolute magnitude of the sum of the convective current density being emitted at the cathode and that returning through the accelerator is constant and is twice the median level.

3) The absolute magnitude of the induced current in the emitter-accelerator region can be represented by

$$\left|J_{e/a}\right| = 2\left|\rho_o v_o\right| + \left|\rho_i v_i\right|\left[\int_{(n)\tau}^{(n+1)\tau} \cos\frac{2\pi t}{6\tau}dt + \int_{(n+3)\tau}^{(n+4)\tau} \cos\frac{2\pi t}{6\tau}dt\right]$$

$$n = 0, 1, 2, 3, \ldots.$$

where $\rho_o v_o$ represents the median, time independent flow and $\rho_i v_i$ represents an alternating component of flow. The magnitude of the induced flow is constant and equal to $2\rho_o v_o$.

Let this model now be examined relative to the action of the oscillator.

1. The model matches the period of the observed

oscillation.

2. The model depends upon suppression of primary electron emission through induced currents of electrons reflected back through the accelerator aperture.

3. The variation in reflected current modulates the emitted current. Any change (such as making the reflector an emitter) that will prevent modulation of the returning electrons will alter or eliminate the oscillation.

Therefore, this model appears to fit the observed results.

Accepting the model leads to the conclusion that the existing relations describing temperature-limited emission must be modified to account for the increase in emission that results from the shift of electrons to higher energy levels as a result of the flow toward the surface. Acceptance of the conclusion that an emitting cathode cannot establish an equilibrium state if electrons are returned a finite period after being emitted suggests that the relations for space-charge-limited emission should also be examined. An expected result would be that the potential minimum will be unstable and that the existing relations describe an average rather than a steady state situation.

SPACE-CHARGE LIMITED OSCILLATION

In the absence of space charge, the potential gradient of a parallel plane diode is

$$\frac{dV}{dx} = \frac{\text{V anode - V cathode}}{\text{anode-to-cathode distance}} = \text{Constant.}$$

With space charge present, however, Poisson's equation in one dimension gives

$$\frac{d^2V}{dx^2} = -\frac{\rho}{\epsilon_o}$$

which indicates that the gradient is no longer linear but has a curvature which is proportional to the space charge density between the electrodes. Since

$$J = \rho v,$$

and

$$eV = \tfrac{1}{2}mv^2,$$

then

$$\frac{d^2V}{dx^2} = \frac{J}{\epsilon_o}\left(\frac{m}{2e}\right)^{\frac{1}{2}} V^{-\frac{1}{2}}$$

Multiplying both sides of the equation by 2dV/dx and

integrating gives

$$\left(\frac{dV}{dx}\right)^2 = \frac{4\ J}{\varepsilon_o}\sqrt{\frac{m}{2e}}\ V^{\frac{1}{2}} + C_1 .$$

At the potential minimum, Vm, dV/dx is zero. For the time being, assume Vm to be zero such that C_1 will be zero. Integrating a second time and solving for the current density gives

$$J = \frac{4\varepsilon_o(2e)^{\frac{1}{2}}\ V^{\frac{3}{2}}}{9\ m^{\frac{1}{2}}\ x^2}$$

if the potential is assumed to be zero at x = o such that C_2 will also be zero. This relation is the familiar Child-Langmuir space-charge law (19). One can solve for V;

$$V = 5{,}680\ J^{2/3}\ x^{4/3} .$$

From previous discussions, J was found to be constant along the path; therefore, a ratio of V at any point, x, to the anode, or accelerator potential, Va, can be formed such that

$$\frac{V}{V_a} = \left(\frac{x}{d}\right)^{\frac{4}{3}},$$

where d is the distance from the potential minimum to the anode. Since $v = f(\sqrt{V})$, then

$$v = \left(\frac{x}{d}\right)^{\frac{2}{3}} v_a .$$

Thus, with space charge present, the velocity of the electron is a function of the 2/3 power of x. The transit time from cathode to anode of a parallel-plane diode, then is

$$\tau = \int_o^d \frac{dx}{v(x)} = \frac{d^{\frac{2}{3}}}{va} \int_o^d x^{-\frac{2}{3}} dx = \frac{3dp}{va}$$

Thus it is seen that the effect of the space charge is to increase the transit time by fifty percent relative to that of a space-charge-free region. Therefore, the effect one would expect in changing from negligible space charge in the case of the temperature limited oscillations to oscillations under full space charge conditions is that the frequency of oscillations for a given accelerator potential would be reduced by a factor of at least $(1.5)^{-1}$.

Child's law for space-charge limited current flow can be written as

$$J = 2.334 \times 10^{-6} \frac{V^{3/2}}{d^2} .$$

Assuming Maxwell-Boltzmann distributions of the emitted electrons, Langmuir's (19) solution to Poisson's equation differs from Child's equations by a conversion function which is determined by the current

level, i.e.,

$$J = 2.334 \times 10^{-6} \frac{(V-Vm)^{\frac{3}{2}}}{(d-dm)^2} \cdot \phi_o(\eta^+)$$

where V is the potential along the direction of electron flow; Vm is the potential of the potential minimum established by the space charge; d is the spacing between the cathode and anode in meters; dm is the distance from the cathode to the potential minimum. The conversion function is of the form

$$\phi_o(\eta^+) = 0.6365 \left[\frac{(\xi^+)^2}{(\eta^+)^{\frac{1}{2}}} \right]$$

where

$$\xi^{\pm} = \int_o^{\eta^{\pm}} \frac{d\eta^{\pm}}{\left[e^{\eta} - 1 \mp e^{\eta} \operatorname{erf}(\eta^{\frac{1}{2}}) \pm \left(\frac{\eta}{\pi}\right)^{\frac{1}{2}} \right]^{\frac{1}{2}}}$$

and

$$\eta^+ = \frac{e(V-Vm)}{kT} = \frac{11,605(V-Vm)}{T},$$

the negative sign designating the space between the cathode and the potential minimum and the plus sign designating the space between the minimum and the anode.

The potential minimum can be considered to be an addition to the work function such that

$$J = J_S \exp\left(\frac{-eVm}{kT}\right)$$

where J is the temperature-limited current; therefore,

$$Vm = \frac{-T}{11{,}605} \ln \frac{J_S}{J} .$$

The distance from the cathode to the potential minimum is given by

$$bm = \frac{\bar{\xi} T^{\frac{3}{4}}}{9.186 \times 10^{5} \; J^{\frac{1}{2}}} .$$

Through the use of tables of $\bar{\xi}$ and η , prepared by Ferris (20), the value of bm can be determined for a parallel plane diode.

The potential distribution of the oscillator under full space charge conditions cannot be accurately determined. However, the location of the potential minimum at a given cathode-current level can be expected to be essentially that of a parallel-plane diode. The potential distribution one would use as a model will be a modification of that shown in Figure 17 to include a potential minimum in front of the emitter. Rack (21) has shown that a system in which cathode current has passed through a transparent accelerator only to be reflected back to the accelerator will establish a potential minimum in the accelerator reflector region deeper than in the cathode-accelerator region. The problem is now one of using these space charge

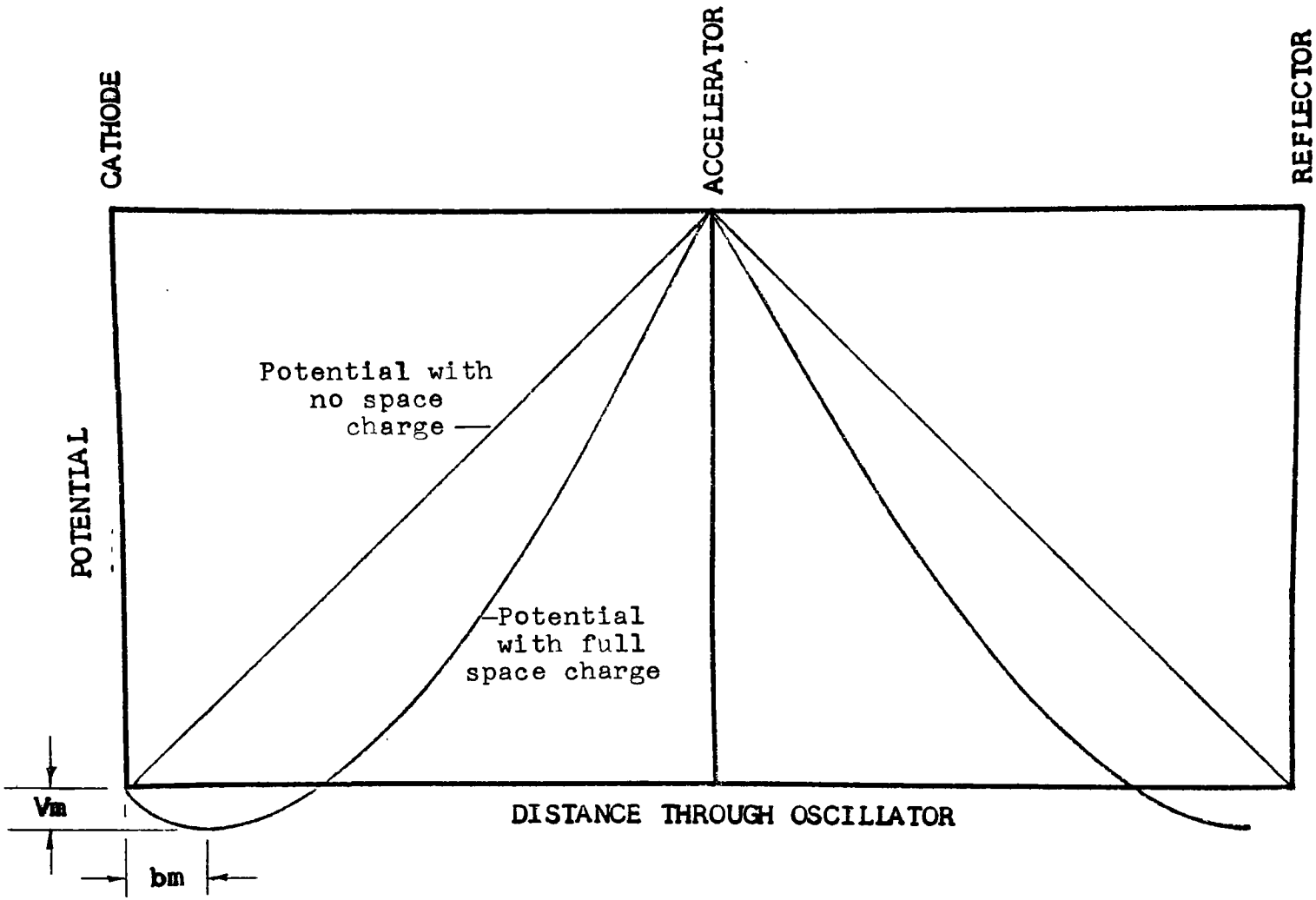

Figure 17. Oscillator Potential with Space Charge Present. The linear potential illustrates a parallel-plane diode assumption with no space charge present. The curved distribution illustrates the effect of full space charge and is the basis for transit time calculations for the space-charge limited case.

characteristics to approximate the potential distribution of the oscillator under full space charge conditions.

If the potential distribution under space-charge-free conditions had been assumed to be linear, rather than that determined by the potential plot, the value of τ would be given by

$$\tau = \left(\frac{2m}{eV}\right)^{\frac{1}{2}} d.$$

The value of τ under this assumption is only found to be 10.6% shorter than that calculated from the accurate potential distribution. Thus, one can get reasonably accurate results by assuming linear distributions then modifying the distributions to account for the fact that the presence of space charge modifies the field such that the transit time will be increased by fifty percent.

Calculation of the transit time for the space-charge-limited case is complicated by the presence of the potential minimum in front of the cathode. The transit time in the cathode-accelerator region can be broken down into two parts: 1) the transit time from cathode to potential minimum and 2) the transit time from potential minimum to the center of the accelerator. To calculate these transit times, the position and depth of the potential minimum had to be calculated

on the basis of measured cathode current densities at several accelerator potentials. This approach is necessary because both the depth and position of the potential minimum vary as a function of cathode current. In the reflector region, the transit time will essentially equal that of the potential minimum to accelerator in the cathode section.

An example of the frequency determination follows: with 230 volts on the accelerator, the cathode current is 16 mA, or a current density of 62 mA per square centimeter. At this current density, the potential minimum is 0.25 volts and the location of the minimum is .015mm in front of the cathode. The transit time of electrons which will just overcome the potential barrier of the minimum under space charge distribution is found to be 1.53×10^{-10} second if a Child's-law distribution is assumed. A Child's-law distribution in the cathode--potential-minimum region is an approximation because the continuous reflection of low energy electrons causes greater concentrations of electrons and, hence, more curvature of the distribution than that resulting from the Child's-law distribution. The transit time from the potential minimum to the center of the accelerator

is 6.67×10^{-10} second. This latter time is also essentially that from the center of the accelerator to the point of reflection. Thus, the transit time in the cathode region is 8.20×10^{-10} second while that of the reflector is 6.67×10^{-10} second. The fundamental frequency should be given by $(6\tau_{ave})^{-1}$, or 224 mHz . Because the transit times are different in the two regions, the tube will create sum and difference frequencies rather than simple harmonics as was the case in the temperature-limited operation. Thus, combining $(6\tau_1)^{-1}$ for the cathode section and $(6\tau_2)^{-1}$ for the reflector section gives a frequency of 450 mHz for the sum and 42 mHz for the difference. Figure 18 is a plot of the calculated and observed frequencies under space-charge-limited conditions.

It can be seen that the predicted and observed frequencies match quite well in spite of the approximations made in assuming initially linear distributions that have been changed into $f(x)^{4/3}$ by the space charge in the cathode--potential-minimum region as well as the other two regions where that assumption is more exact.

Thus the results indicate that the oscillation mechanism for the temperature-limited and space-charge limited operation is the same.

TABLE II

OBSERVED FREQUENCIES AND ACCELERATOR POTENTIALS FOR SPACE-CHARGE LIMITED OPERATION.

Accelerator Potential Volts	Radiation Frequency Megahertz
21	77
24	83
25	104
50	104
57	211
110	225
150	197
165	182
230	55
230	211
300	470

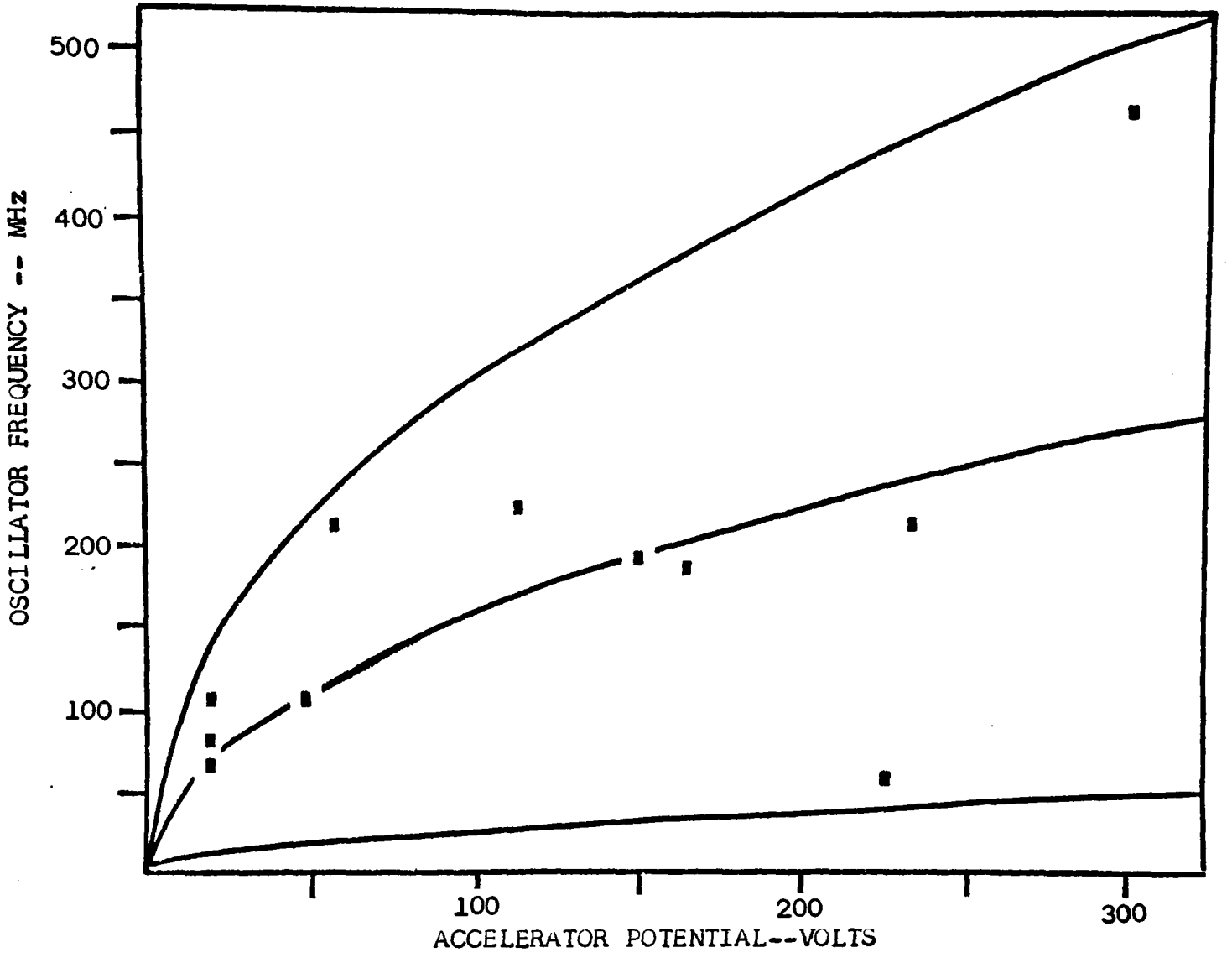

Figure 18. Calculated and Observed Frequencies under Space-Charge Conditions.

One can also hypothesize that reflections of electrons by the potential minimum will cause the potential minimum to be unstable and that a very high frequency pulsation of period 2τ, where τ is the transit time from the cathode to the potential minimum, will exist in space-charge limited emissions. The frequency of this pulsation, however, would be so high that special equipment would have to be obtained to detect it.

CONCLUSIONS

The results of this investigation indicate that space charge oscillations will occur when a thermionic cathode emits electrons into a potential well which reflects the electrons back to the cathode after a finite period. The oscillations are essentially independent of the circuit impedances. The frequency of the oscillation is an inverse function of the transit-time of the well.

The model that fits the results best suggests that the current density being emitted by a thermionic cathode is influenced by the current induced in the emitter by the flow of electrons in the interelectrode space. The model indicates that the flow of electrons away from the emitter induces an electron flow within the emitter such that electrons are raised to higher energy levels in the flow direction. This transition to higher energy levels causes the emitted current density to be higher than that predicted by conventional calculations. When electrons are returned to the cathode, induced flow reduces the energy of

electrons in the flow direction such that the emitted current is lower than that predicted by conventional calculations.

A further inference from the model is that the potential minimum of thermionic cathode is inherently unstable as a result of modulation of the primary emission by electrons reflected by the potential minimum.

If the model is valid, an example of useful devices which could be based on enhancement of the effect would be high-frequency, voltage-tunable, vacuum tube oscillators. Investigation of the potential use of the effect in solid-state devices might also prove valuable.

APPENDIX I

Effects of Initial Velocities

The initial velocity of the emitted electrons can be evaluated by calculating the expected value of the velocity distribution at the surface of the emitter (18):

$$\langle w|x\rangle = \int w f(w|x)\,dw$$

$$= 2\pi^{-3/2}\int \frac{w \exp(-w^2)\,dw}{\left[1 \pm \operatorname{erf}(\eta^{1/2})\right]}$$

$$= i\left[\pi^{1/2}\exp\eta\left\{1 \pm \operatorname{erf}(\eta^{1/2})\right\}\right]^{-1}$$

where i is the unit vector in the x direction, and w is the dimensionless velocity; i. e.,

$$w = \left(\frac{m}{2kT}\right)^{1/2} v \ .$$

At the surface of the temperature-limited emitter $\eta = 0$. Therefore,

$$\langle w|x_c\rangle = i\pi^{-1/2}$$

$$\langle v|x_c\rangle = i\left(\frac{2kT}{\pi m}\right)^{1/2} \ .$$

The temperature of the cathode under the temperature-limited conditions was $735^{o}K$. Thus, the mean initial velocity of the electrons is approximately 10^{5} meters/second. The effect of the initial velocity is to reduce the transit time by only 0.2 percent at the lowest accelerator voltage at which oscillations were observed. The effects of initial velocity were, therefore, neglected.

REFERENCES

1. H. Barkhausen and K. Kurz, "Shortest Waves Obtainable with Valve Generators," Phys. Zeit., Vol. 21, pp. 1-6, January, 1920.

2. E. W. Gill and J. H. Morrell, Phil. Mag., Vol. 44, pp. 161-178, (1922).

3. W. H. Moore, "Electron Oscillations Without Tuned Circuits," Proceedings of the IRE, Vol. 22, pp. 1021-1036, (1934).

4. A. Scheibe, Ann. Dev. Phys., Vol. 73, No. 4, pp. 54-88, (1924).

5. H. E. Hollmann, Ann. Dev. Phys., Vol. 86. pp. 129-187, (1928).

6. T. V. Jonescu, Comptes Rendus, Vol. 193, pp. 575-577, October 12, (1931).

7. B. J. Thompson and P. D. Zotto, "An Electron Oscillator with Plane Electrodes," Proc. of the IRE, Vol. 21, pp. 1374-1385, December, 1934.

8. L. F. Dytrt, "Barkhausen-Kurz Oscillator Operation with Positive Plate Potentials," Proc. of the IRE, Vol. 23, pp. 2'1-2'3, March, 1935.

9. F. B. Llewellyn, "Vacuum Tube Electronics at Ultra-High Frequencies," Proc. of the IRE, Vol. 21, pp. 1532-1574; November, 1933.

10. F. B. Llewellyn, "Note on Vacuum Tube Electronics at Ultra-High Frequencies," Proc. of the IRE, Vol. 22, pp. 112-127; February, 1935.

11. J. J. Ebers, "Retarding-Field Oscillator," Proc. of the IRE, Vol. 40, pp. 138-145, February, 1952.

12. D. Hoognoed and A. J. Huart, "Improvements in Television Receivers," Electronic Applications, Vol. 17, pp. 41-55, (1957).

13. W. L. Carl, "Barkhausen Oscillations in the UHF Region--Part I," IEEE Transactions on Broadcast and Television Receivers, Vol. 10, pp. 33-37, May, 1964.

14. L. J. Maginn, "Barkhausen Oscillation in the UHF Region--Part II," IEEE Transactions on Broadcast and Television Receivers, Vol. 10, pp. 38-41, May, 1964.

15. W. L. Carl, "Sheet Beam Electron Discharge Device with Means for Preventing Unwanted Oscillation of the Beam," U. S. Patent 3,424,933, January, 1969.

16. S. Ramo, "Currents Induced by Electron Motion," Proc. of the IRE, Vol. 27, pp. 584-585, September, 1939.

17. R. Sproull, Modern Physics, John Wiley and Sons, Inc., New York, 1967 , 2nd ed., Chap. 12, p. 437.

18. P. A. Lindsay, "Velocity Distribution in Electron Streams," in "Advances in Electronics and Electron Physics," Academic Press, New York, N. Y., Vol. 13; 1960.

19. I. Langmuir, "The Effect of Space Charge and Initial Velocities on the Potential Distribution and Thermionic Current Between Parallel Plane Electrodes," Phys. Rev., Vol. 21, pp. 419-435; April, 1923.

20. W. Ferris, "Some Characteristics of Diodes with Oxide Coated Cathodes," RCA Rev., Vol. 10, pp. 134-149; March, 1949.

21. A. J. Rack, "Effect of Space Charge and Transit Time on the Shot Noise in Diodes," Bell Sys. Tech J., Vol. 17, pp. 592-619, October, 1938.